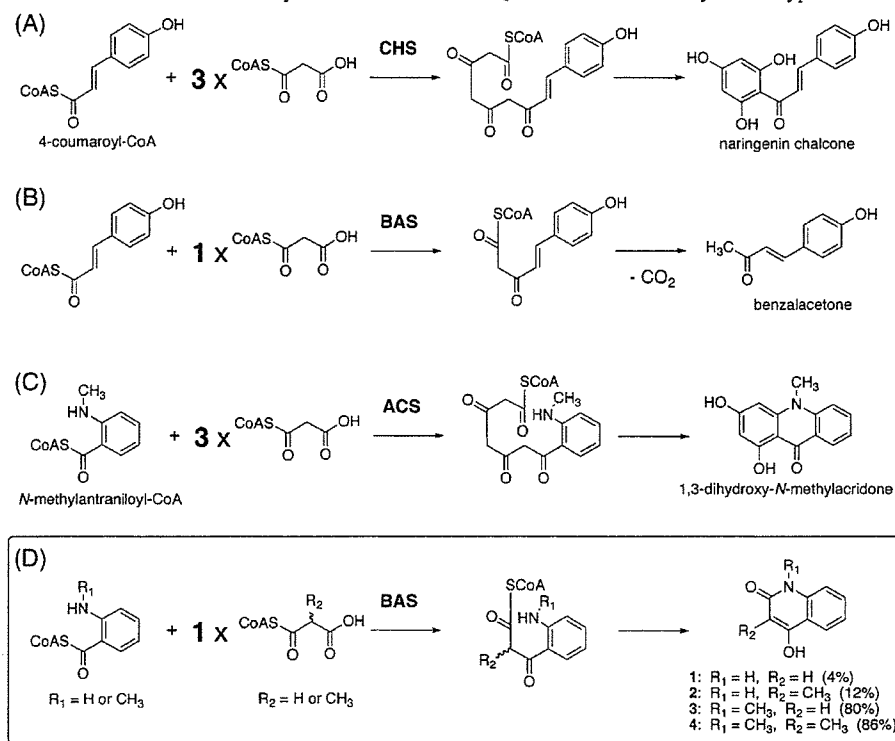


Scheme 1. Formation of Polyketides and Acridone/Quinolone Alkaloids by Plant Type III PKSs^a



^a Yield (%) of quinolone production under the standard assay conditions (see Supporting Information).

novel alkaloidal scaffold produced by a CHS superfamily type III PKS (Scheme 1D). The quinolone alkaloids⁶ have been investigated as *N*-methyl-D-aspartate⁷ (NMDA) and serotonin 5-HT₃⁸ receptor antagonists. Moreover, they are also important intermediates in the chemical synthesis of alkaloids.⁹

Anthranilic acid has been postulated to be a key intermediate in the biosynthesis of quinolone and acridone alkaloids, which occur in the greatest abundance in plants from the family of Rutaceae (Figure 1).¹⁰ In fact, acridone synthase (ACS) from *Ruta graveolens* is a plant-specific type III PKS that selects *N*-methylantraniloyl-CoA as a starter and performs three condensations with malonyl-CoA to

produce 1,3-dihydroxy-*N*-methylacridone (a tetraketide) (Scheme 1C);¹¹ however, the enzyme involved in the biosynthesis of quinolone alkaloids has not been identified yet. Interestingly, the chalcone-forming CHS and other type III PKSs, except ACS, do not accept the shorter and the bulkier *N*-methylantraniloyl-CoA as a starter unit despite their promiscuous substrate specificity. Although the *Medicago sativa* CHS F215S mutant has been shown to accept *N*-methylantraniloyl-CoA to produce an unnatural novel tetraketide lactone after three condensations with malonyl-CoA,^{5c} enzymatic formation of a quinolone alkaloid (a diketide) by type III PKSs including mutants of *R. graveolens* ACS¹¹ has not been reported so far.

R. palmatum BAS is the enzyme that catalyzes one-step condensation with malonyl-CoA to produce a diketide benzalacetone.³ When recombinant *R. palmatum* BAS functionally expressed in *Escherichia coli* was incubated with

(5) (a) Schütz, R.; Heller, W.; Hahlbrock, K. *J. Biol. Chem.* **1983**, *258*, 6730–6734. (b) Zaubier, K. W. M.; Leser, J.; Berger, T.; Hoffe, A. J. P.; Schröder, G.; Verpoorte, R.; Schröder, J. *Phytochemistry* **1998**, *49*, 1945–1951. (c) Jez, J. M.; Bowman, M. E.; Noel, J. P. *Proc. Natl. Acad. Sci. U.S.A.* **2002**, *99*, 5319–5324. (d) Samappito, S.; Page, J.; Schmidt, J.; De-Eknamkul, W.; Kutchan, T. M. *Planta* **2002**, *216*, 64–71. (e) Samappito, S.; Page, J. E.; Schmidt, J.; De-Eknamkul, W.; Kutchan, T. M. *Phytochemistry* **2003**, *62*, 313–323.

(6) Two-step synthesis of 4-hydroxyquinolinones from anthranilate derivatives by a tellurium-triggered cyclization reaction has been recently reported; see: Dittmer, D. C.; Li, Q.; Avilov, D. V. *J. Org. Chem.* **2005**, *70*, 4682–4686.

(7) (a) Rowley, M.; Kulagowski, J. J.; Watt, A. P.; Rathbone, D.; Stevenson, G. I.; Carling, R. W.; Baker, R.; Marshall, G. R.; Kemp, J. A.; Foster, A. C.; Grimwood, S.; Hargreaves, R.; Hurley, C.; Saywell, K. L.; Tricklebank, M. D.; Leeson, P. D. *J. Med. Chem.* **1997**, *40*, 4053–4068. (b) Zhou, Z.-L.; Navratil, J. M.; Cai, S. X.; Whittemore, E. R.; Espitia, S. A.; Hawkins, J. E.; Tran, M.; Woodward, R. M.; Weber, E.; Keana, J. F. W. *Bioorg. Med. Chem.* **2001**, *9*, 2061–2071.

(8) Hayashi, H.; Miwa, Y.; Ichikawa, S.; Yoda, N.; Miki, I.; Ishii, A.; Kono, M.; Yasuzawa, T.; Suzuki, F. *J. Med. Chem.* **1993**, *36*, 617–626.

(9) (a) Watters, W. H.; Ramachandran, V. N. *J. Chem. Res. Synop.* **1997**, 184–185. (b) Majumdar, K. C.; Choudhury, P. K. *Synth. Commun.* **1993**, *23*, 1087–1100. (c) Grundon, M. F.; Ramachandran, V. N. *Tetrahedron Lett.* **1985**, *26*, 4253–4256. (d) Corral, R. A.; Orazi, O. O.; Autino, J. C. *Tetrahedron Lett.* **1983**, *24*, 2359–2360. (e) Reisch, J.; Mueller, M.; Mester, L. Z. *Naturforsch. B: Anorg. Chem., Org. Chem.* **1981**, *36B*, 1176–1179.

(10) Dewick, P. M. *Medicinal Natural Products, A Biosynthetic Approach*, 2nd ed.; Wiley: West Sussex, 2002.

(11) (a) Junghanns, K. T.; Kneusel, R. E.; Baumert, A.; Mainer, W.; Groger, D.; Matern, U. *Plant Mol. Biol.* **1995**, *27*, 681–692. (b) Lukacin, R.; Springob, K.; Urbanke, C.; Ernwein, C.; Schröder, G.; Schröder, J.; Matern, U. *FEBS Lett.* **1999**, *448*, 135–140. (c) Springob, K.; Lukacin, R.; Ernwein, C.; Groning, I.; Matern, U. *Eur. J. Biochem.* **2000**, *267*, 6552–6559. (d) Lukacin, R.; Schreiner, S.; Matern, U. *FEBS Lett.* **2001**, *508*, 413–417. (e) Lukacin, R.; Schreiner, S.; Silber, K.; Matern, U. *Phytochemistry* **2005**, *66*, 277–284.

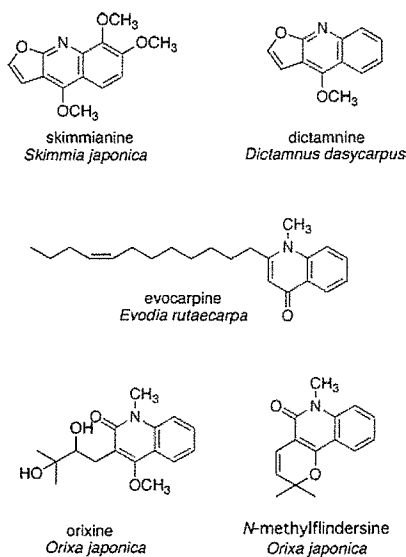


Figure 1. Naturally occurring quinoline alkaloids derived from 4-hydroxy-2(1H)-quinolones from Rutaceae plants.¹²

N-methylanthraniloyl-CoA (or anthraniloyl-CoA) and malonyl-CoA (or methylmalonyl-CoA) as substrates, the enzyme efficiently afforded 4-hydroxy-2(1H)-quinolones (**1**–**4**) as a single product (Scheme 1D). The condensation products were not detected in control experiments performed with a boiled enzyme preparation. The spectroscopic data (LC-ESIMS, UV, and ¹H NMR) of the compounds were characteristic of those of the quinolone alkaloids and completely identical with those of authentic compounds.⁶ For example, the LC-ESIMS spectrum of 4-hydroxy-1-methyl-2(1H)-quinolone (**3**) gave a parent ion peak [M + H]⁺ at *m/z* 176, indicating the structure of a diketide. The ¹H NMR of **3** obtained from a large-scale enzyme reaction (0.4 mg from 2 mg of *N*-methylanthraniloyl-CoA and 4 mg of malonyl-CoA) showed one methyl singlet (δ 3.52) in addition to one vinyl proton (δ 5.86) and four aromatic protons (δ 7.89–7.17), supporting that the heterocyclic system adopts the more stable 4-hydroxy-2(1H)-quinolone form. Confirmation of the structure was finally obtained by direct comparison with the commercially available authentic compound. These quinolone alkaloids have never been isolated from *R. palmatum* (Polygonaceae).

Interestingly, the enzyme reaction with the anthraniloyl-CoA proceeds without the “decarboxylation” step, and the amide formation immediately follows the condensation reactions of *N*-methylanthraniloyl-CoA (or anthraniloyl-CoA) and malonyl-CoA (or methylmalonyl-CoA) (Scheme 1D). This was also the case for the conversion of benzoyl-CoA (i.e., without the methylamino group of *N*-methylanthraniloyl-CoA) to 6-phenyl-4-hydroxy-2-pyrone (a triketide) by *R. palmatum* BAS.^{3b} Furthermore, the quinolone formation activity showed a broad pH optimum within a range of pH 6.0–8.5. Thus, the pH change did not affect the product profile; formation of triketides or other polyketides was not detected in the reaction mixture. In contrast, the pH optimum

for the formation of benzalacetone was reported to be at maximum within a range of pH 8.0–8.5. It should be noted that *R. palmatum* BAS exhibited a dramatic change from benzalacetone to triketide pyrone production at acidic pH.^{3b}

For the quinolone production, the best yield (86% under the standard assay conditions) was obtained with the combination of *N*-methylanthraniloyl-CoA and methylmalonyl-CoA. Notably, both esters are nonphysiological substrates for *R. palmatum* BAS. On the other hand, a combination of anthraniloyl-CoA and malonyl-CoA afforded only 4% yield. Steady-state enzyme kinetics for the formation of 4-hydroxy-1,3-dimethyl-2(1H)-quinolone (**4**) revealed $K_M = 23.7 \mu\text{M}$ and $k_{\text{cat}} = 1.48 \text{ min}^{-1}$ for *N*-methylanthraniloyl-CoA, which was comparable with those for the formation of benzalacetone, the normal product of the enzyme; $K_M = 10.0 \mu\text{M}$ and $k_{\text{cat}} = 1.79 \text{ min}^{-1}$ for 4-coumaroyl-CoA. This strongly suggests the presence of a not yet identified novel type III PKS that produces quinolone alkaloids¹² from the CoA thioester of anthranilic acid (Figure 1).

In *R. graveolens* ACS, the residues Ser132, Ala133, and Val265 (numbering in *M. sativa* CHS) have been proposed to play a critical role for the selection of *N*-methylanthraniloyl-CoA as a starter substrate and for the formation of the acridone alkaloid.^{11d} Indeed, an ACS triple mutant (S132T/A133S/V265F) has been shown to yield an enzyme that was functionally identical with CHS.^{11d} However, interestingly, two of the residues are not conserved in *R. palmatum* BAS (S132L/V265F) that accepted the anthraniloyl starter. On the other hand, the diketide-forming activity of the BAS enzyme is derived from the characteristic substitution of the active-site gatekeeper Phe215; the conformationally flexible residue conserved in all the known type III PKSs is uniquely replaced with nonaromatic Leu in BAS.³ Although the BAS L215F mutant has been shown to recover chalcone-forming activity to produce chalcone after three condensations with malonyl-CoA,^{3b} the mutant did not produce the tetraketide acridone from the anthraniloyl starter but instead just yielded the diketide quinolone. These results suggest subtle differences of the active-site structure between *R. palmatum* BAS and *R. graveolens* ACS.

In summary, the present work describes the first enzymatic synthesis of 4-hydroxy-2(1H)-quinolones. Manipulation of the functionally divergent CHS superfamily type III PKSs by nonphysiological substrates thus provides an efficient method for production of pharmaceutically important plant alkaloids.

Acknowledgment. This work was supported by the PRESTO program from the Japan Science and Technology Agency, a Grant-in-Aid for Scientific Research (Nos. 18510190 and 17310130), and the COE21 program from the Ministry of Education, Culture, Sports, Science and Technology, Japan.

Supporting Information Available: Materials and methods. This material is available free of charge via the Internet at <http://pubs.acs.org>.

OL0625233

(12) Michael, J. P. *Nat. Prod. Rep.* **2004**, *21*, 650–668.



Enzymatic formation of an unnatural methylated triketide by plant type III polyketide synthases

Tsuyoshi Abe,^a Hisashi Noma,^a Hiroshi Noguchi^a and Ikuro Abe^{a,b,*}

^a*School of Pharmaceutical Sciences and the 21st Century COE Program, University of Shizuoka, 52-1 Yada, Shizuoka 422-8526, Japan*

^b*PRESTO, Japan Science and Technology Agency, Kawaguchi, Saitama 332-0012, Japan*

Received 25 September 2006; revised 2 October 2006; accepted 3 October 2006
Available online 20 October 2006

Abstract—Octaketide synthase, a novel plant-specific type III polyketide synthase from *Aloe arborescens*, efficiently accepted (2*RS*)-methylmalonyl-CoA as a sole substrate to produce 6-ethyl-4-hydroxy-3,5-dimethyl-2-pyrone. On the other hand, a tetraketide-producing chalcone synthase from *Scutellaria baicalensis* and a diketide-producing benzalacetone synthase from *Rheum palmatum* also yielded the unnatural methylated C₉ triketide pyrone as a single product by sequential decarboxylative condensations of three molecules of (2*RS*)-methylmalonyl-CoA.

© 2006 Elsevier Ltd. All rights reserved.

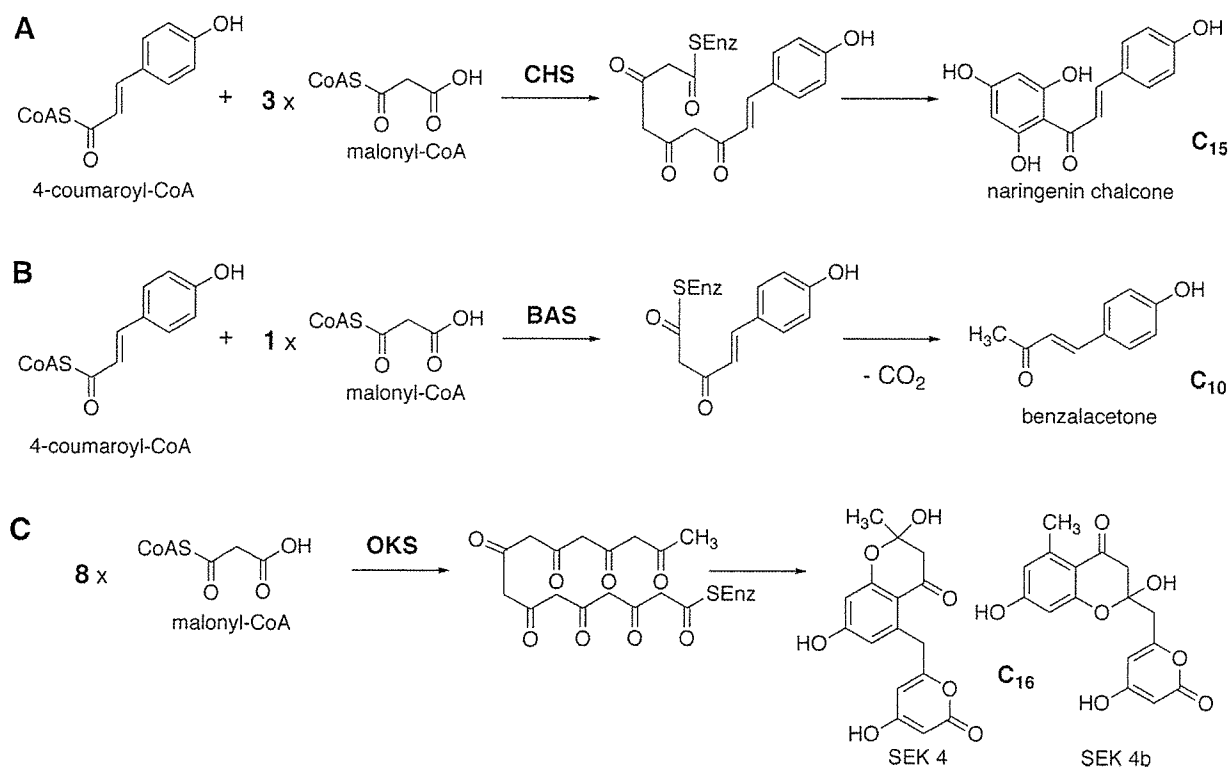
The broad substrate tolerance and catalytic potential of the chalcone synthase (CHS) (EC 2.3.1.74) superfamily of type III polyketide synthases (PKSs) are remarkable.^{1,2} Octaketide synthase (OKS) is a recently reported novel plant-specific type III PKS from *Aloe arborescens*, catalyzing sequential condensation of eight molecules of malonyl-CoA to produce aromatic C₁₆ octaketides SEK4 and SEK4b (Scheme 1), the longest polyketides known to be synthesized by the structurally simple homodimeric type III PKS.³ Like other type III PKSs,^{4,5} *A. arborescens* OKS exhibits unusually broad, promiscuous substrate specificities; the enzyme accepts a variety of non-physiological substrates, including aromatic and aliphatic CoA thioesters, to generate an array of chemically and structurally distinct unnatural polyketides.³ Here we now report enzyme reactions using (2*RS*)-methylmalonyl-CoA, instead of malonyl-CoA, as a sole substrate. It was interesting to test whether the octaketides-producing *A. arborescens* OKS accepts (2*RS*)-methylmalonyl-CoA, with an additional bulky methyl group, as a *starter* substrate and extends an intermediate to produce novel octaketides.

In previous studies, we have demonstrated that a tetraketide-producing *Scutellaria baicalensis* CHS^{4a} and a diketide-producing *Rheum palmatum* benzalacetone synthase (BAS)⁶ accepted (2*RS*)-methylmalonyl-CoA as an *extender* substrate to produce unnatural polyketides.^{4d,e} Further, it has been reported that *Pinus strobus* CHS2 carried out a one-step condensation of a diketide *N*-acetylcysteamine thioester and (2*RS*)-methylmalonyl-CoA to produce a methylated triketide styrylpyrone.⁷

Recombinant *A. arborescens* OKS was expressed in *E. coli*, and purified by Ni-chelate affinity chromatography as described before.^{3,8} When incubated with (2*RS*)-methylmalonyl-CoA as a sole substrate, *A. arborescens* OKS efficiently afforded a single product (UV λ_{\max} 292 nm) (Fig. 1A).⁹ The LC–ESIMS spectrum gave a parent ion peak [M+H]⁺ at *m/z* 169, suggesting that the reaction had terminated after two condensations of (2*RS*)-methylmalonyl-CoA, and in MS/MS (precursor ion at *m/z* 169), the fragment at *m/z* 125 corresponded to [M+H–CO₂]⁺, suggesting the presence of an α -pyrone ring. Further, the ¹H NMR spectrum of the product obtained from a large scale enzyme reaction (80% yield from 4 mg of (2*RS*)-methylmalonyl-CoA) revealed signals at δ 2.54 (q, 2H, *J* = 7.5 Hz), 1.21 (t, 3H, *J* = 7.5 Hz), 1.98 (s, 3H), and 1.96 (s, 3H), indicating the presence of one ethyl

Keywords: Type III polyketide synthase; Chalcone synthase; Octaketide synthase; Benzalacetone synthase; Methylated triketide pyrone.

* Corresponding author. Tel./fax: +81 54 264 5662; e-mail: abei@ys7.u-shizuoka-ken.ac.jp



Scheme 1. Proposed mechanism for the formation of (A) naringenin chalcone from 4-coumaroyl-CoA and three molecules of malonyl-CoA by CHS, (B) benzalacetone from 4-coumaroyl-CoA and one molecule of malonyl-CoA by BAS, and (C) SEK4 and SEK4b from eight molecules of malonyl-CoA by OKS.

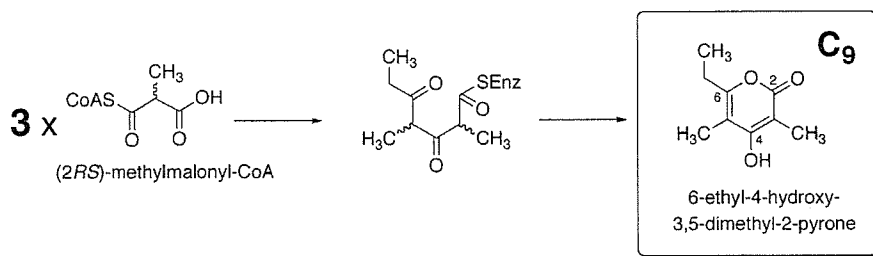
group and two methyl groups. The spectroscopic data (LC-ESIMS, UV, MS, and ¹H NMR)¹⁰ were identical with those of 6-ethyl-4-hydroxy-3,5-dimethyl-2-pyrone,¹¹ which was chemically synthesized by condensation of three molecules of propionyl chloride.^{11a} The structure of the enzyme reaction product was thus confirmed to be 6-ethyl-4-hydroxy-3,5-dimethyl-2-pyrone, which was consistent with biogenetic reasoning (Scheme 2). Interestingly, the compound has been reported from the fungus *Emericella heterothallica*,^{11b} however, it has never been isolated from any plant sources including *A. arborescens*.

The C₁₆ octaketides-producing *A. arborescens* OKS, normally catalyzing condensation of eight molecules of malonyl-CoA, thus accepted the bulky (2*RS*)-methylmalonyl-CoA, both as a *starter* and an *extender* substrate, and carried out sequential decarboxylative condensation to produce the methylated C₉ triketide pyrone (Scheme 2). This is the first demonstration of the enzymatic formation of 6-ethyl-4-hydroxy-3,5-dimethyl-2-pyrone by the structurally simple plant-specific type III PKS.

In addition to *A. arborescens* OKS, a C₁₅ tetraketide-producing *S. baicalensis* CHS and a C₁₀ diketide-producing *R. palmatum* BAS also accepted (2*RS*)-methylmalonyl-CoA as a *starter* substrate and efficiently yielded the unnatural methylated C₉ triketide pyrone as a

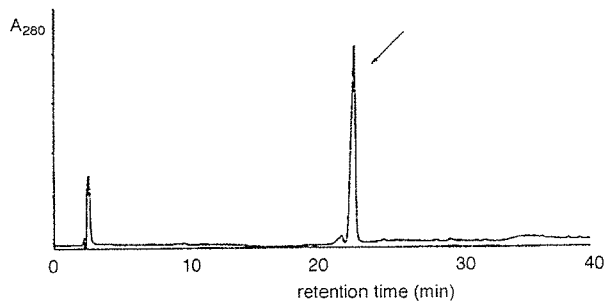
single product by sequential decarboxylative condensations of three molecules of (2*RS*)-methylmalonyl-CoA (Fig. 1B and C).^{8,9} Here, CHS is a pivotal enzyme for flavonoid biosynthesis, catalyzing the formation of naringenin chalcone from 4-coumaroyl-CoA and three molecules of malonyl-CoA (Scheme 1A), whereas BAS carries out a one-step decarboxylative condensation of 4-coumaroyl-CoA with malonyl-CoA to produce a diketide benzalacetone (Scheme 1B). On the other hand, it has been reported that a bacterial modular type I PKS (a cell-free system of recombinant 6-deoxyerythronolide B synthase; DEBS 1 + TE) produced 6-ethyl-4-hydroxy-3,5-dimethyl-2-pyrone from propionyl-CoA, as a *starter*, and (2*RS*)-methylmalonyl-CoA, as an *extender*, in the absence of NADPH.¹² In this case, (2*RS*)-methylmalonyl-CoA was not accepted as a *starter* substrate by the bacterial modular type I PKS.

It is remarkable that the plant-specific type III PKSs accept (2*RS*)-methylmalonyl-CoA, with an additional bulky methyl group, both as a *starter* and an *extender* substrate, and catalyze the formation of the non-physiological methylated C₉ triketide pyrone. This demonstrated the further tremendous catalytic potential of the CHS-superfamily type III PKS enzymes. Manipulation of the functionally divergent type III PKSs by utilizing non-physiological substrates as active-site probes would thus lead to further production of unnatural

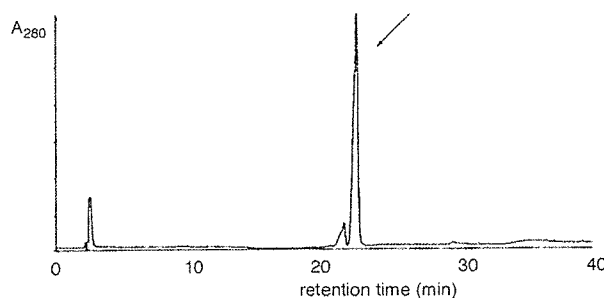


Scheme 2. Formation of 6-ethyl-4-hydroxy-3,5-dimethyl-2-pyrone by sequential decarboxylative condensations of three molecules of (2*RS*)-methylmalonyl-CoA.

A *A. arborescens* OKS



B *S. baicalensis* CHS



C *R. palmatum* BAS

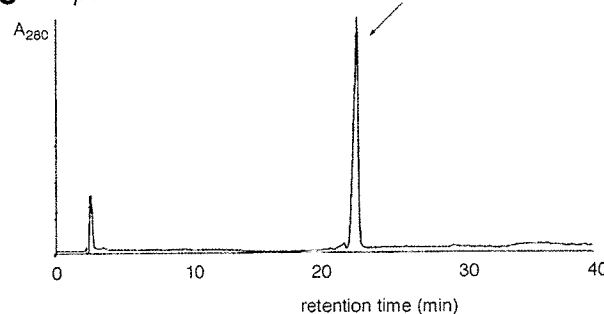


Figure 1. HPLC elution profiles of enzyme reaction products of (A) *A. arborescens* OKS, (B) *S. baicalensis* CHS, and (C) *R. palmatum* BAS.

novel polyketides, which is now in progress in our laboratories.

Acknowledgements

This work was supported by the PRESTO program from Japan Science and Technology Agency, Grant-in-

Aid for Scientific Research (Nos. 18510190 and 17310130), Cooperation of Innovative Technology and Advanced Research in Evolutional Area (CITY AREA, the Central Shizuoka Area), and the COE21 program from the Ministry of Education, Culture, Sports, Science and Technology, Japan.

References and notes

- For recent reviews, see: (a) Schröder, J. In *Comprehensive Natural Products Chemistry*; Elsevier: Oxford, 1999; Vol. 2, pp 749–771; (b) Austin, M. B.; Noel, J. P. *Nat. Prod. Rep.* **2003**, *20*, 79–110.
- (a) Ferrer, J. L.; Jez, J. M.; Bowman, M. E.; Dixon, R. A.; Noel, J. P. *Nat. Struct. Biol.* **1999**, *6*, 775–784; (b) Jez, J. M.; Ferrer, J. L.; Bowman, M. E.; Dixon, R. A.; Noel, J. P. *Biochemistry* **2000**, *39*, 890–902; (c) Jez, J. M.; Noel, J. P. *J. Biol. Chem.* **2000**, *275*, 39640–39646; (d) Jez, J. M.; Bowman, M. E.; Noel, J. P. *Biochemistry* **2001**, *40*, 14829–14838; (e) Tropf, S.; Kärcher, B.; Schröder, G.; Schröder, J. *J. Biol. Chem.* **1995**, *270*, 7922–7928; (f) Suh, D. Y.; Fukuma, K.; Kagami, J.; Yamazaki, Y.; Shibuya, M.; Ebizuka, Y.; Sankawa, U. *Biochem. J.* **2000**, *350*, 229–235; (g) Austin, M. B.; Bowman, M. E.; Ferrer, J.-L.; Schröder, J.; Noel, J. P. *Chem. Biol.* **2004**, *11*, 1179–1194; (h) Abe, I.; Watanabe, T.; Morita, H.; Kohno, T.; Noguchi, H. *Org. Lett.* **2006**, *8*, 499–502.
- Abe, I.; Oguro, S.; Utsumi, Y.; Sano, Y.; Noguchi, H. *J. Am. Chem. Soc.* **2005**, *127*, 12709–12716.
- (a) Abe, I.; Morita, H.; Nomura, A.; Noguchi, H. *J. Am. Chem. Soc.* **2000**, *122*, 11242–11243; (b) Morita, H.; Takahashi, Y.; Noguchi, H.; Abe, I. *Biochem. Biophys. Res. Commun.* **2000**, *279*, 190–195; (c) Morita, H.; Noguchi, H.; Schröder, J.; Abe, I. *Eur. J. Biochem.* **2001**, *268*, 3759–3766; (d) Abe, I.; Takahashi, Y.; Noguchi, H. *Org. Lett.* **2002**, *4*, 3623–3626; (e) Abe, I.; Takahashi, Y.; Lou, W.; Noguchi, H. *Org. Lett.* **2003**, *5*, 1277–1280; (f) Abe, I.; Watanabe, T.; Noguchi, H. *Phytochemistry* **2004**, *65*, 2447–2453; (g) Oguro, S.; Akashi, T.; Ayabe, S.; Noguchi, H.; Abe, I. *Biochem. Biophys. Res. Commun.* **2004**, *325*, 561–567; (h) Abe, I.; Utsumi, Y.; Oguro, S.; Noguchi, H. *FEBS Lett.* **2004**, *562*, 171–176; (i) Abe, I.; Utsumi, Y.; Oguro, S.; Morita, H.; Sano, Y.; Noguchi, H. *J. Am. Chem. Soc.* **2005**, *127*, 1362–1363; (j) Abe, I.; Watanabe, T.; Noguchi, H. *Proc. Jpn. Acad., Ser. B.* **2006**, *81*, 434–440.
- (a) Schütz, R.; Heller, W.; Hahlbrock, K. *J. Biol. Chem.* **1983**, *258*, 6730–6734; (b) Zuurbier, K. W. M.; Leser, J.; Berger, T.; Hofte, A. J. P.; Schröder, G.; Verpoorte, R.; Schröder, J. *Phytochemistry* **1998**, *49*, 1945–1951; (c) Jez, J. M.; Bowman, M. E.; Noel, J. P. *Proc. Natl. Acad. Sci. U.S.A.* **2002**, *99*, 5319–5324; (d) Samappito, S.; Page, J.; Schmidt, J.; De-Eknamkul, W.; Kutchan, T. M. *Planta* **2002**, *216*, 64–71; (e) Samappito, S.; Page, J. E.; Schmidt,

- J.; De-Eknamkul, W.; Kutchan, T. M. *Phytochemistry* **2003**, *62*, 313–323.
6. (a) Abe, I.; Takahashi, Y.; Morita, H.; Noguchi, H. *Eur. J. Biochem.* **2001**, *268*, 3354–3359; (b) Abe, I.; Sano, Y.; Takahashi, Y.; Noguchi, H. *J. Biol. Chem.* **2003**, *278*, 25218–25226.
7. Schröder, J.; Raiber, S.; Berger, T.; Schmidt, A.; Schmidt, J.; Soares-Sello, A. M.; Bardshiri, E.; Strack, D.; Simpson, T. J.; Veit, M.; Schröder, G. *Biochemistry* **1998**, *37*, 8417–8425.
8. Recombinant *A. arborescens* OKS,³ *S. baicalensis* CHS,^{4a} and *R. palmatum* BAS⁶ with an additional hexahistidine tag at the C-terminal were expressed in *E. coli*, and purified by Ni-chelate affinity chromatography as described before. The purified enzymes showed the following K_M and k_{cat} values; OKS (95.0 μM and 0.094 min^{-1} for malonyl-CoA), CHS (36.1 μM and 1.26 min^{-1} for 4-coumaroyl-CoA), and BAS (10.0 μM and 1.79 min^{-1} for 4-coumaroyl-CoA).
9. The reaction mixture contained (2*RS*)-methylmalonyl-CoA (108 μM) and the purified recombinant enzyme (20 μg) in 100 mM potassium phosphate buffer (500 μL , pH 8.0), containing 1 mM EDTA. Incubations were carried out at 30 °C for 12 h, and stopped by addition of 20% HCl (50 μL). The products were then extracted with ethyl acetate (1 mL), and separated by reverse-phase HPLC (column, TSK-gel ODS-80Ts, 4.6 \times 150 mm, Tosoh Co. Ltd, Japan; flow rate, 0.8 mL/min). Gradient elution was performed with H₂O and MeOH, both containing 0.1% TFA: 0–5 min, 30% MeOH; 5–17 min, linear gradient from 30% to 60% MeOH; 17–25 min, 60% MeOH; 25–27 min, linear gradient from 60% to 70% MeOH. For large-scale enzyme reactions, (2*RS*)-methylmalonyl-CoA (4 mg) was incubated with purified recombinant enzyme (10 mg) in 100 mM phosphate buffer (40 mL, pH 8.0), containing 1 mM EDTA at 30 °C for 18 h.
10. LC-ESIMS: m/z 169 [M+H]⁺. MS/MS (precursor ion at m/z 169): m/z 125 [M+H-CO₂]⁺. UV: λ_{max} 292 nm. ¹H NMR (400 MHz, CD₃OD): δ 2.54 (q, 2H, $J = 7.5$ Hz), 1.98 (s, 3H), 1.96 (s, 3H), 1.21 (t, 3H, $J = 7.5$ Hz). MS (FAB⁺): m/z 168 [M]⁺, 140, 125 [M+H-CO₂]⁺, 113. The spectroscopic data were identical with those reported in the literature.¹¹
11. (a) Osman, M. A.; Seibl, J.; Oretsch, E. *Helv. Chem. Acta* **1977**, *60*, 3007–3011; (b) Kawahara, N.; Nakajima, S.; Kawai, K. *Phytochemistry* **1989**, *28*, 1546–1548.
12. Pieper, R.; Luo, G.; Cane, D. E.; Khosla, C. *J. Am. Chem. Soc.* **1995**, *117*, 11373–11374.

Crystallization and preliminary crystallographic analysis of a novel plant type III polyketide synthase that produces pentaketide chromone

Hiroyuki Morita,^a Shin Kondo,^b
Tsuyoshi Abe,^c Hiroshi
Noguchi,^c Shigetoshi Sugio,^{b*}
Ikuro Abe^{c,d*} and Toshiyuki
Kohno^{a*}

^aMitsubishi Kagaku Institute of Life Sciences (MITILS), 11 Minamiooya, Machida, Tokyo 194-8511, Japan, ^bZOEGENE Corporation, 1000 Kamoshida, Aoba, Yokohama, Kanagawa 227-8502, Japan,

^cSchool of Pharmaceutical Sciences and the COE21 Program, University of Shizuoka, Shizuoka 422-8526, Japan, and ^dPRESTO, Japan Science and Technology Agency, Kawaguchi, Saitama 332-0012, Japan

Correspondence e-mail:
ssugio@rc.m-kagaku.co.jp,
abe@ys7.u-shizuoka-ken.ac.jp,
tkohno@libra.ls.m-kagaku.co.jp

Received 14 June 2006

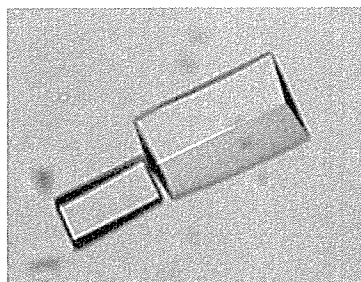
Accepted 30 July 2006

Pentaketide chromone synthase (PCS) from *Aloe arborescens* is a novel plant-specific type III polyketide synthase that catalyzes the formation of 5,7-dihydroxy-2-methylchromone from five molecules of malonyl-CoA. Recombinant PCS expressed in *Escherichia coli* was crystallized by the hanging-drop vapour-diffusion method. The crystals belonged to space group $P2_1$, with unit-cell parameters $a = 73.2$, $b = 88.4$, $c = 70.0$ Å, $\alpha = \gamma = 90.0$, $\beta = 95.6^\circ$. Diffraction data were collected to 1.6 Å resolution using synchrotron radiation at BL24XU of SPring-8.

1. Introduction

The chalcone synthase (CHS; EC 2.3.1.74) superfamily of type III polyketide synthases (PKSs) are structurally and mechanistically distinct from the modular type I and the dissociated type II PKSs of bacterial origin. The 40–45 kDa enzymes, which form simple homodimers, catalyze sequential decarboxylative condensations of malonyl-CoA with a CoA-linked starter molecule without the involvement of the acyl carrier protein to produce a variety of biologically active plant secondary metabolites (Schröder, 1999; Austin & Noel, 2003). For example, CHS, the pivotal enzyme in flavonoid biosynthesis, produces naringenin chalcone through the sequential condensation of 4-coumaroyl-CoA with three C_2 units from malonyl-CoA. On the other hand, 2-pyrone synthase (2PS) from *Gerbera hybrida* selects acetyl-CoA as a starter and carries out only two condensations with malonyl-CoA to produce triacetic acid lactone (TAL). Recent crystallographic and site-directed mutagenesis studies have begun to reveal the structural and functional details of the type III PKSs, which share a common three-dimensional overall fold and active-site architecture with a conserved Cys-His-Asn catalytic triad (Ferrer *et al.*, 1999; Jez *et al.*, 2000; Austin *et al.*, 2004). The polyketide-formation reaction is initiated by the starter molecule loading at the active-site Cys, which is followed by malonyl-CoA decarboxylation, polyketide chain elongation and cyclization of the polyketide intermediate. In principle, the remarkable functional diversity of the CHS-superfamily type III PKSs is derived from only a small modification of the active-site geometry (Jez *et al.*, 2000; Abe, Oguro *et al.*, 2005; Abe *et al.*, 2006).

Pentaketide chromone synthase (PCS) from *Aloe arborescens* is a novel plant-specific type III PKS that produces 5,7-dihydroxy-2-methylchromone from five molecules of malonyl-CoA (Fig. 1a; Abe, Utsumi *et al.*, 2005). The aromatic pentaketide is a biosynthetic precursor of the anti-asthmatic furochromones kehellin and visnagin. The amino-acid sequence of *A. arborescens* PCS shares 50–60% identity with those of the CHS-superfamily enzymes from other plants: 58% identity with *Medicago sativa* CHS and 57% identity with *G. hybrida* 2PS. Sequence comparisons revealed that the Cys-His-Asn catalytic triad and most of the CHS active-site residues are well conserved in *A. arborescens* PCS: however, the conserved Thr197, Gly256 and Ser338 in the CHSs (numbering according to *M. sativa* CHS; Ferrer *et al.*, 1999), which are uniquely altered in a number of divergent type III PKSs, are replaced with Met, Leu and Val, respectively, in *A. arborescens* PCS. The three residues lining the active-site cavity are also missing in *G. hybrida* 2PS (T197L/G256L/S338I; Jez *et al.*, 2000) and in *A. arborescens* octaketide synthase



© 2006 International Union of Crystallography
All rights reserved

(OKS; T197G/G256L/S338V; Abe, Oguro *et al.*, 2005). Remarkably, the replacement of Met207 of *A. arborescens* PCS (corresponding to Thr197 in the CHSs) with the less bulky Gly yielded a mutant enzyme that efficiently catalyzes the successive condensation of eight molecules of malonyl-CoA to produce SEK4 and SEK4b (Fig. 1b; Abe, Utsumi *et al.*, 2005). The octaketides are known to be the products of the minimal type II PKS for actinorhodin (*act* from *Streptomyces coelicolor*) and the longest polyketides ever generated by the structurally simple type III PKS. The pentaketide-forming PCS was thus functionally transformed into an octaketide-producing enzyme by the single amino-acid substitution. The functional diversity of the type III PKS was thus demonstrated to be evolved from the simple steric modulation of a single chemically inert residue lining the active-site cavity (Abe, Oguro *et al.*, 2005; Abe *et al.*, 2006). To further clarify the intimate three-dimensional structural details of the enzyme-catalyzed processes and to elucidate the structure–function relationship of the type III PKS enzymes, we now report the crystallization and preliminary crystallographic analysis of *A. arborescens* PCS.

2. Experimental

2.1. Expression and purification

A pET-41a(+) vector encoding full-length *A. arborescens* PCS (Abe, Utsumi *et al.*, 2005) was used as a template to amplify the PCS gene by PCR, using 5'-GCGCCCGGGAATGAGTTCACCTCTCAACG-3' as a sense primer that introduces a *Sma*I restriction site and 5'-GCGCTCGAGTTACATGAGAGGCAGGCTGTGAA-3' as an antisense primer that introduces a *Xho*I restriction site. The amplified DNA fragment was digested with *Sma*I/*Xho*I and was cloned into the *Sma*I/*Sal*I sites of a modified pET24a(+) expression vector (Novagen) for expression as a glutathione *S*-transferase (GST) fusion protein at the N-terminus. Between GST and PCS, a PreScission Protease (Amersham Biosciences) cleavage site (LEVLFQGP) was introduced. After confirmation of the sequence, the resultant expression plasmid was transformed into *Escherichia coli* BL21(DE3) pLysS.

Protein expression, extraction and initial purification by Glutathione Sepharose 4B affinity chromatography (Amersham Bio-

sciences) were carried out as previously reported, except for the use of PreScission Protease digestion to remove the GST tag (Abe, Utsumi *et al.*, 2005). The resultant PCS protein thus contains three additional residues (GPG) at the N-terminal flanking region derived from the PreScission Protease recognition sequence. After affinity purification and GST-tag removal, the protein solution containing the recombinant PCS was diluted fivefold with 50 mM HEPES–NaOH buffer pH 7.0 containing 5% glycerol and 2 mM DTT and was then applied onto a Resource-Q column (Amersham Biosciences). The column was washed with HEPES–NaOH buffer containing 50 mM NaCl and the protein was subsequently eluted using a linear gradient of 50–200 mM NaCl. The protein solution was further purified to homogeneity by chromatography on Superdex 200HR (10/100 GL; Amersham Biosciences) and was concentrated to 10 mg ml⁻¹ in 20 mM HEPES–NaOH pH 7.0 buffer containing 100 mM NaCl and 2 mM DTT. The typical yield of protein was about 0.5 mg per litre of culture.

2.2. Crystallization and X-ray data collection

Initial crystallization attempts were carried out at 293 K using an original 96-condition screening set (ZOEGENE Corporation) with the sitting-drop vapour-diffusion method. Crystals were observed under many crystallization conditions and one of the more promising crystallization conditions was further optimized. Finally, diffraction-quality crystals were obtained at 293 K in 100 mM Tris–HCl buffer pH 8.5 containing 14% (*w/v*) PEG 8000 and 350 mM KF using the hanging-drop vapour-diffusion method. The crystallization drops were prepared by mixing 0.5 µl protein solution and an equal volume of reservoir solution and were equilibrated against 500 µl reservoir solution. The crystals appeared reproducibly within 2 d and grew to average dimensions of approximately 0.2 × 0.1 × 0.1 mm (Fig. 2).

The crystals were transferred to the reservoir solution with 20% (*v/v*) glycerol as a cryoprotectant, picked up in a nylon loop and then flash-cooled at 100 K in a nitrogen-gas stream. X-ray diffraction data were collected from a single crystal at SPring-8 beamline BL24XU using a Rigaku R-AXIS V imaging-plate area detector with 180 frames. The 1° oscillation images were recorded with exposure times of 48 s. The wavelength of the synchrotron radiation was

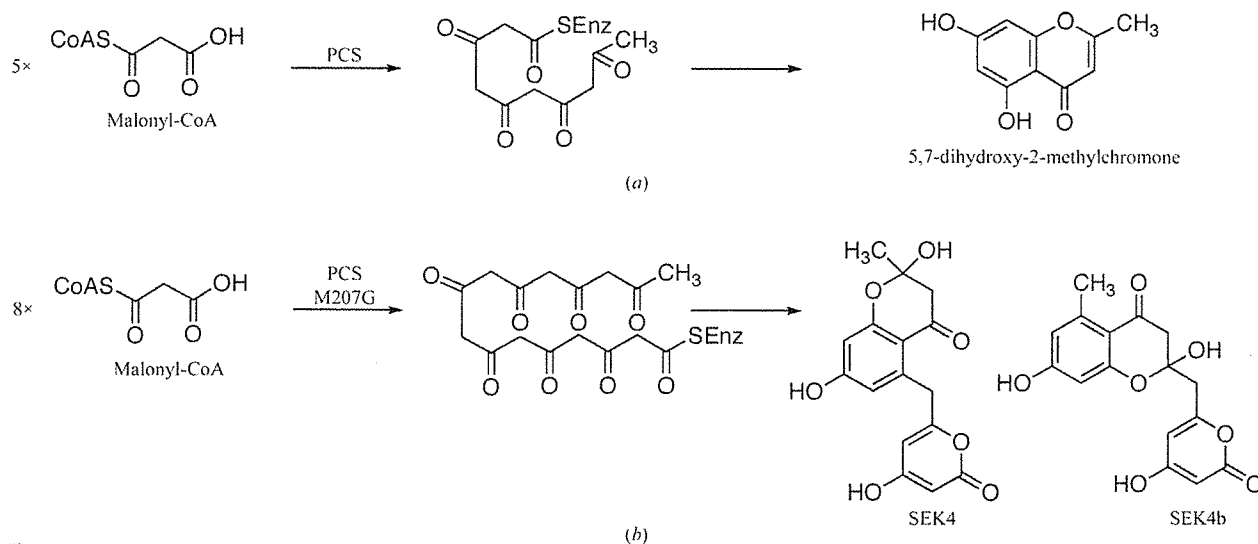


Figure 1 Proposed mechanism for the formation of (a) 5,7-dihydroxy-2-methylchromone from five molecules of malonyl-CoA by PCS and (b) SEK4 and SEK4b from eight molecules of malonyl-CoA by the PCS M207G mutant.

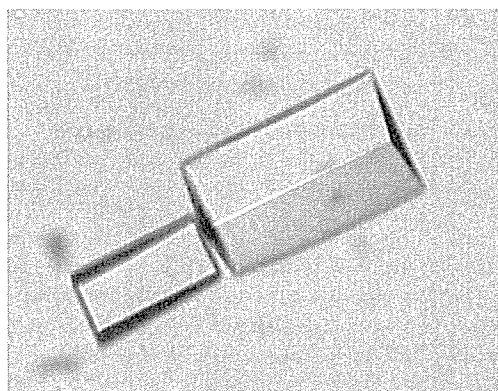


Figure 2
Crystals of *A. arborescens* PCS grown by the hanging-drop method. The dimensions of the largest crystal were approximately $0.2 \times 0.1 \times 0.1$ mm.

0.82656 \AA and the distance between the crystal and the detector was 340 mm. Data were indexed, integrated and scaled with the *HKL-2000* program package (Otwinowski & Minor, 1997).

3. Results and discussion

Recombinant PCS was heterologously expressed in *E. coli* as a fusion protein with GST at the N-terminus. After cleavage of the GST tag, the purified enzyme migrated as a single band with a molecular weight of 44 kDa on SDS-PAGE, which is in good agreement with the calculated value of 44 779 Da. A gel-filtration experiment gave a molecular weight of 88 kDa, suggesting that *A. arborescens* PCS is a homodimeric enzyme, as is the case for other known type III PKSS. A complete data set was collected to 1.6 \AA resolution. Detailed data-processing statistics are shown in Table 1. From the diffraction data collection, the space group was determined to be monoclinic $P2_1$, with unit-cell parameters $a = 73.2$, $b = 88.4$, $c = 70.0 \text{ \AA}$, $\alpha = \gamma = 90.0$, $\beta = 95.6^\circ$. With two monomers in the asymmetric unit, the Matthews coefficient (V_M ; Matthews, 1968) was calculated to be $2.5 \text{ \AA}^3 \text{ Da}^{-1}$; the estimated solvent content is thus 49.0%, which is in the range normally observed for protein crystals.

The preliminary crystal structure of PCS was determined by the molecular-replacement method, with the reported crystal structure of *G. hybrida* 2PS (PDB code 1ec0; Jez *et al.*, 2000) as a search model, using the *EPMR* program (Kissinger *et al.*, 1999). The initial model had an *R* factor of 41% and showed an unknown compound within

Table 1
Data-collection statistics.

Values in parentheses are for the highest resolution shell.

Space group	$P2_1$
Unit-cell parameters	
a (\AA)	73.2
b (\AA)	88.4
c (\AA)	70.0
β ($^\circ$)	95.6
Resolution (\AA)	30.0–1.6 (1.66–1.60)
Unique reflections	116521
Redundancy	3.7 (3.8)
Completeness (%)	99.9 (100)
$\langle I(\sigma I) \rangle$	33.5 (8.4)
R_{sym}^\dagger (%)	6.9 (23.0)

$^\dagger R_{\text{sym}} = \sum_h \sum_i |I(h)_i - \langle I(h) \rangle| / \sum_h \sum_i I(h)_i$, where $I(h)$ is the intensity of reflection h , \sum_h is the sum over all reflections and \sum_i is the sum over i measurements of reflection h .

the traditional CoA-binding tunnel. Further refinements and analyses of the structure are in progress. Simultaneously, we are attempting to crystallize the PCS M207G mutant. Structural analyses of both proteins will provide valuable insights into the molecular mechanism of the functionally diverse type III PKSS.

This work was supported in part by a grant from the National Project on Protein Structural and Functional Analyses.

References

- Abe, I., Oguro, S., Utsumi, Y., Sano, Y. & Noguchi, H. (2005). *J. Am. Chem. Soc.* **127**, 12709–12716.
- Abe, I., Utsumi, Y., Oguro, S., Morita, H., Sano, Y. & Noguchi, H. (2005). *J. Am. Chem. Soc.* **127**, 1362–1363.
- Abe, I., Watanabe, T., Morita, H., Kohno, T. & Noguchi, H. (2006). *Org. Lett.* **8**, 499–502.
- Austin, M. B., Izumikawa, M., Bowman, M. E., Udwyary, D. W., Ferrer, J. L., Moore, B. S. & Noel, J. P. (2004). *J. Biol. Chem.* **279**, 45162–45174.
- Austin, M. B. & Noel, J. P. (2003). *Nat. Prod. Rep.* **20**, 79–110.
- Ferrer, J. L., Jez, J. M., Bowman, M. E., Dixon, R. A. & Noel, J. P. (1999). *Nature Struct. Biol.* **6**, 775–784.
- Jez, J. M., Austin, M. B., Ferrer, J., Bowman, M. E., Schroder, J. & Noel, J. P. (2000). *Chem. Biol.* **7**, 919–930.
- Kissinger, C. R., Gehlhaar, D. K. & Fogel, D. B. (1999). *Acta Cryst.* **D55**, 484–491.
- Matthews, B. W. (1968). *J. Mol. Biol.* **33**, 491–497.
- Otwinowski, Z. & Minor, W. (1997). *Methods Enzymol.* **276**, 307–326.
- Schröder, J. (1999). *Comprehensive Natural Products Chemistry*, Vol. 2, edited by D. E. Cane, pp. 749–771. Oxford: Elsevier.

Engineered Biosynthesis of Plant Polyketides: Manipulation of Chalcone Synthase

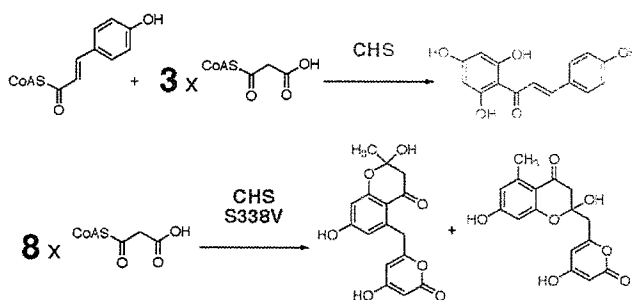
Ikuro Abe,^{*,†,§} Tatsuya Watanabe,[†] Hiroyuki Morita,[‡] Toshiyuki Kohno,[‡] and Hiroshi Noguchi[†]

School of Pharmaceutical Sciences and the COE 21 Program, University of Shizuoka, Shizuoka 422-8526, Japan, PRESTO, Japan Science and Technology Agency, Kawaguchi, Saitama 332-0012, Japan, and Mitsubishi Kagaku Institute of Life Sciences (MITILS), Machida, Tokyo 194-8511, Japan

abei@ys7.u-shizuoka-ken.ac.jp

Received December 1, 2005

ABSTRACT



Chalcone synthase (CHS) is a plant-specific type III polyketide synthase catalyzing condensation of 4-coumaroyl-CoA with three molecules of malonyl-CoA. Surprisingly, it was demonstrated that S338V mutant of *Scutellaria baicalensis* CHS produced octaketides SEK4/SEK4b from eight molecules of malonyl-CoA. Further, the octaketides-forming activity was dramatically increased in a CHS triple mutant (T197G/G256L/S338T). The functional conversion is based on the simple steric modulation of a chemically inert residue lining the active-site cavity.

The chalcone synthase (CHS) superfamily of type III polyketide synthases (PKSs) share a common three-dimensional overall fold with a conserved Cys-His-Asn catalytic triad to produce structurally diverse polyphenols with remarkable biological activities.¹ CHS is the well-characterized plant-specific type III PKS that produces naringenin chalcone (4,2',4',6'-tetrahydroxychalcone), the biosynthetic precursor of flavonoids, through a sequential condensation of 4-coumaroyl-CoA with three molecules of malonyl-CoA (Figure 1A).² In an *in vitro* enzyme reaction, CHS also produces bis-noryangonin (BNY) and 4-couma-

royltriacetic acid lactone (CTAL) as early-released derailment byproducts (Figure 1A).² On the other hand, recently reported octaketide synthase (OKS) from *Aloe arborescens* catalyzes condensation of eight molecules of malonyl-CoA to produce a 1:4 mixture of octaketide SEK4 and SEK4b (Figure 1B),^{3b} the shunt products of the minimal type II PKS from

[†] University of Shizuoka.

[§] PRESTO, Japan Science and Technology Agency.

[‡] Mitsubishi Kagaku Institute of Life Sciences.

(1) For recent reviews, see: (a) Schröder, J. In *Comprehensive Natural Products Chemistry*; Elsevier: Oxford, 1999; Vol. 2, pp 749–771. (b) Austin, M. B.; Noel, J. P. *Nat. Prod. Rep.* **2003**, *20*, 79–110.

(2) (a) Ferrer, J. L.; Jez, J. M.; Bowman, M. E.; Dixon, R. A.; Noel, J. P. *Nat. Struct. Biol.* **1999**, *6*, 775–784. (b) Jez, J. M.; Ferrer, J. L.; Bowman, M. E.; Dixon, R. A.; Noel, J. P. *Biochemistry* **2000**, *39*, 890–902. (c) Jez, J. M.; Noel, J. P. *J. Biol. Chem.* **2000**, *275*, 39640–39646. (d) Jez, J. M.; Bowman, M. E.; Noel, J. P. *Biochemistry* **2001**, *40*, 14829–14838. (e) Tropsch, S.; Kärcher, B.; Schröder, G.; Schröder, J. *J. Biol. Chem.* **1995**, *270*, 7922–7928. (f) Suh, D. Y.; Fukuma, K.; Kagami, J.; Yamazaki, Y.; Shibuya, M.; Ebizuka, Y.; Sankawa, U. *Biochem. J.* **2000**, *350*, 229–235. (g) Jez, J. M.; Bowman, M. E.; Noel, J. P. *Proc. Natl. Acad. Sci. U.S.A.* **2002**, *99*, 5319–5324. (h) Austin, M. B.; Bowman, M. E.; Ferrer, J.-L.; Schröder, J.; Noel, J. P. *Chem. Biol.* **2004**, *11*, 1179–1194. (i) Abe, I.; Sano, Y.; Takahashi, Y.; Noguchi, H. *J. Biol. Chem.* **2003**, *278*, 25218–25226.

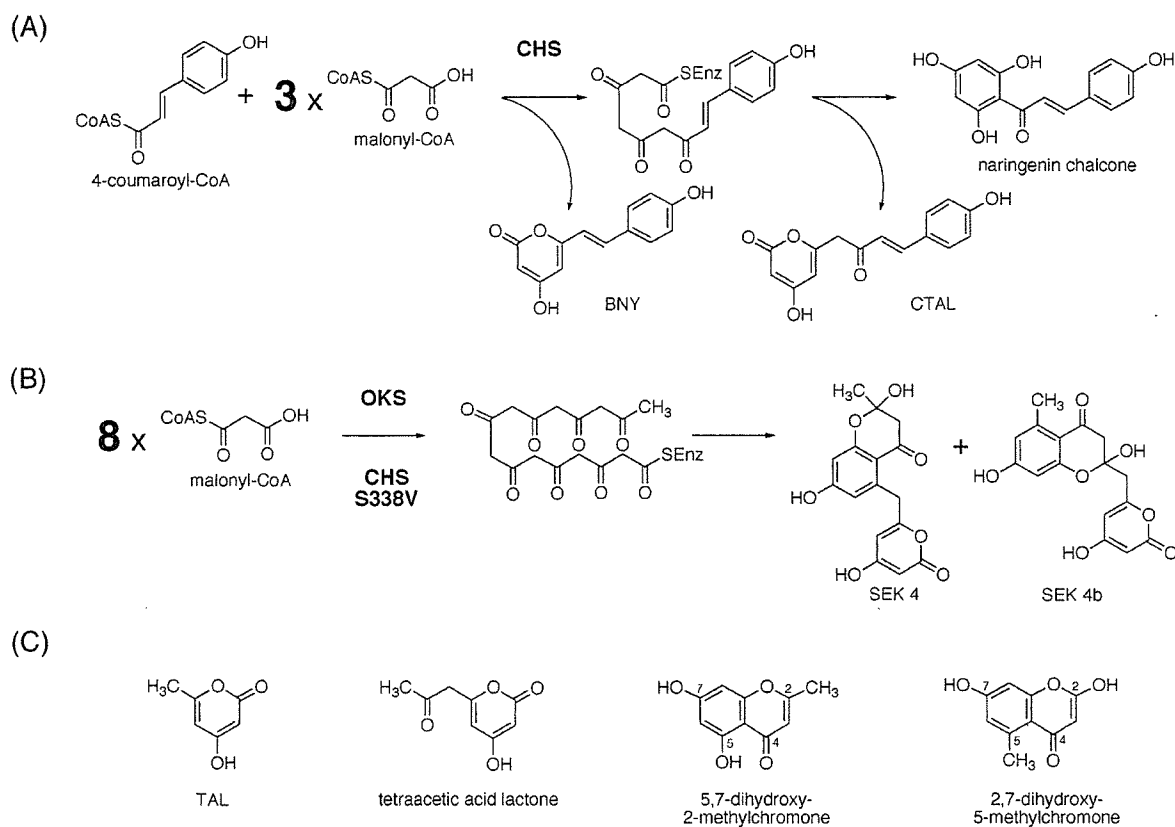


Figure 1. Formation of (A) chalcone by CHS, (B) SEK4/SEK4b by OKS (and CHS S338V), and (C) other polyketide products.

*Streptomyces coelicolor*⁴ and the longest polyketides generated by the structurally simple type III PKS.³ In *A. arbore-scens* OKS, the CHS's active-site residues Thr197, Gly256, and Ser338 (numbering in *Medicago sativa* CHS^{2a}) are uniquely replaced with Gly, Leu, and Val, respectively (T197G/G256L/S338V).^{3b} Interestingly, the three residues lining the active-site cavity are sterically altered in a number of functionally divergent type III PKSs including *A. arbore-scens* pentaketide chromone synthase (PCS) (T197M/G256L/S338V)^{3a}, *Rheum palmatum* aloesone synthase (T197A/G256L/S338T),⁵ and *Gerbera hybrida* 2-pyrone synthase (2PS) (T197L/G256L/S338I).⁶ These chemically inert residues have been shown to control starter substrate and product specificity by steric modulation of the active-site cavity in *M. sativa* CHS and in *G. hybrida* 2PS.^{2d,6b} Further, in

previous papers, we reported that the residue 197 determines the polyketide chain length and product specificities in the octaketide-producing *A. arbore-scens* OKS and the pentaketide-producing *A. arbore-scens* PCS.³

To further study the structure–function relationship between CHS and OKS enzyme, here we constructed a series of *Scutellaria baicalensis* CHS⁷ mutants in which the three residues were changed from those in CHS to those in OKS (T197G, G256L, and S338V), and investigated the mechanistic consequences of the mutations using 4-coumaroyl-CoA and/or malonyl-CoA as substrates.

Interestingly, in the absence of the coumaroyl starter, both wild-type and the mutant *S. baicalensis* CHSs initiated decarboxylative condensation of malonyl-CoA, but most of the polyketide chain elongation reactions were terminated at the triketide stage to predominantly produce triacetic acid lactone (TAL) (Figure 2A). This is in good agreement with an earlier report that mutation of *M. sativa* CHS at the residues (T197L, G256L, and S338I) resulted in functional

(3) (a) Abe, I.; Utsumi, Y.; Oguro, S.; Morita, H.; Sano, Y.; Noguchi, H. *J. Am. Chem. Soc.* **2005**, *127*, 1362–1363. (b) Abe, I.; Oguro, S.; Utsumi, Y.; Sano, Y.; Noguchi, H. *J. Am. Chem. Soc.* **2005**, *127*, 12709–12716.

(4) (a) Fu, H.; Ebert-Khosla, S.; Hopwood, D. A.; Khosla, C. *J. Am. Chem. Soc.* **1994**, *116*, 4166–4170. (b) Fu, H.; Hopwood, D. A.; Khosla, C. *Chem. Biol.* **1994**, *1*, 205–210.

(5) (a) Abe, I.; Utsumi, Y.; Oguro, S.; Noguchi, H. *FEBS Lett.* **2004**, *562*, 171–176. (b) Abe, I.; Watanabe, T.; Lou, W.; Noguchi, H. *FEBS J.* **2006**, *273*, 208–218.

(6) (a) Eckermann, S.; Schröder, G.; Schmidt, J.; Strack, D.; Edrada, R. A.; Helariutta, Y.; Elomaa, P.; Kotilainen, M.; Kilpeläinen, I.; Proksch, P.; Teeri, T. H.; Schröder, J. *Nature* **1998**, *396*, 387–390. (b) Jez, J. M.; Austin, M. B.; Ferrer, J.; Bowman, M. E.; Schröder, J.; Noel, J. P. *Chem. Biol.* **2000**, *7*, 919–930.

(7) (a) Abe, I.; Morita, H.; Nomura, A.; Noguchi, H. *J. Am. Chem. Soc.* **2000**, *122*, 11242–11243. (b) The deduced amino acid sequences of *S. baicalensis* CHS showed 77.4% (302/389) identity with those of *M. sativa* CHS and 60.4% (235/389) identity with *A. arbore-scens* OKS. The recombinant enzyme with an additional hexahistidine tag at the C-terminal was expressed in *E. coli* and purified by Ni-chelate chromatography as described before.^{7a} The wild-type enzyme showed $K_M = 36.1 \mu\text{M}$ and $k_{cat} = 1.26 \text{ min}^{-1}$ for 4-coumaroyl-CoA.

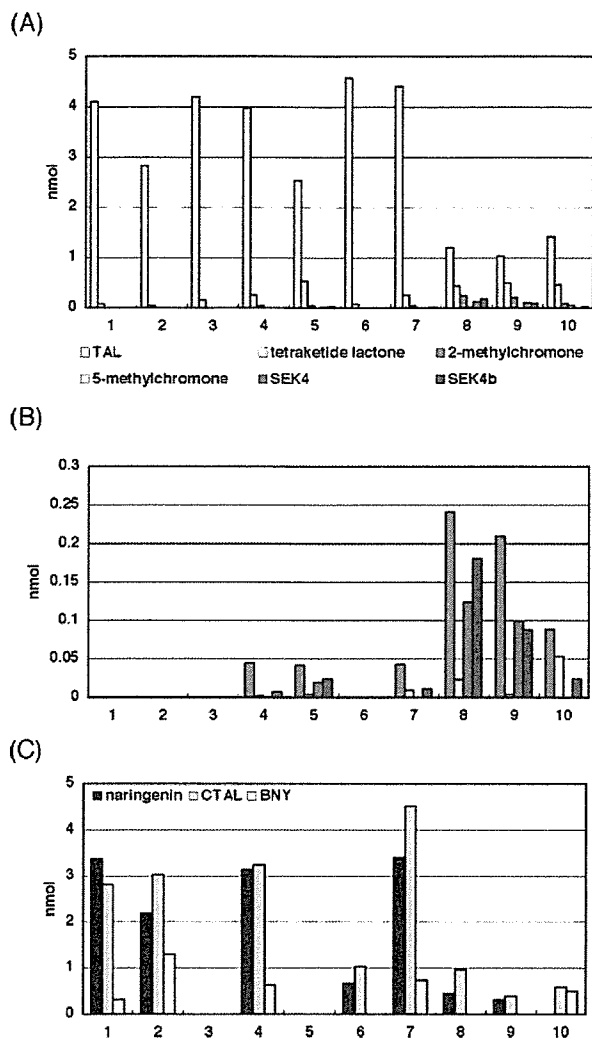


Figure 2. Distribution pattern of polyketides produced by CHS mutants: (A) from malonyl-CoA (all products), (B) from malonyl-CoA (pentaketides and octaketides), (C) from 4-coumaroyl-CoA/malonyl-CoA. (1) wild-type, (2) T197G, (3) G256L, (4) S338V, (5) G256L/S338V, (6) T197G/G256L, (7) T197G/S338V, (8) T197G/G256L/S338V, (9) T197A/G256L/S338V, (10) T197M/G256L/S338V.

conversion into a TAL-producing enzyme.^{6b} However, very surprisingly, careful examination of the enzyme reaction products revealed that CHS S338V mutant yielded a trace amount of SEK4/SEK4b in addition to 5,7-dihydroxy-2-methylchromone,^{3a} 2,7-dihydroxy-5-methylchromone,^{3b} and tetracetic acid lactone^{3b} (Figures 1C and 2B). It was thus for the first time demonstrated that CHS could be engineered to produce longer octaketides by the single amino acid replacement. Furthermore, the SEK4/SEK4b-forming activity was dramatically increased in an OKS-like triple mutant (T197G/G256L/S338V) (Figure 2B). On the other hand, in the presence of 4-coumaroyl-CoA in the assay mixture, most of the *S. baicalensis* CHS mutants still accepted the coumaroyl starter to produce chalcone, whereas interestingly

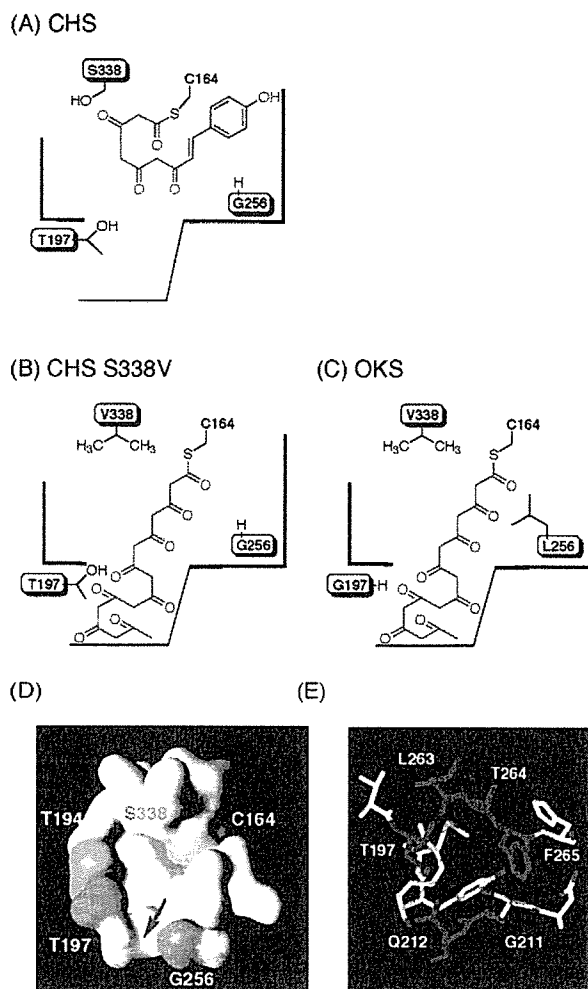


Figure 3. Schematic representation of the active-site architecture of (A) CHS, (B) CHS S338V mutant, and (C) *A. arborescens* OKS. (D) CHS's active-site cavity and an entrance to a novel buried pocket, and (E) the entrance of the buried pocket (a putative polyketide elongation tunnel) that extends into the "floor" of the active-site cavity.

G256L and G256L/S338V mutant did not afford any products from 4-coumaroyl-CoA (Figure 2C).

Out of the three point mutations tested (T197G, G256L, and S338V), the hydrophobic replacement S338V is critical for production of the longer chain polyketides including SEK4/SEK4b.⁸ In contrast, T197G and G256L mutant did not produce any malonate-derived polyketides except TAL and tetraacetic acid lactone. On the basis of the published X-ray crystal structure of *M. sativa* CHS at 1.56 Å resolution,^{2a} the residue 338 is located in proximity of the catalytic Cys164 at the "ceiling" of the active-site cavity and plays a crucial role in the polyketide chain elongation

(8) *S. baicalensis* CHS S338I (2PS-like) mutant also produced a trace amount of SEK4/SEK4b, whereas S338A, S338F, and S338T (ALS-like) mutant only produced the pentaketide chromones. Interestingly, S338C mutant did not produce any malonate-derived polyketides except TAL.

reactions. Further interestingly, the crystal structure also revealed presence of an additional buried pocket that extends into the “floor” of the traditional CHS active site (Figure 3).⁹ Presumably, the **S338V** mutation provided steric guidance so that the linear polyketide intermediate extends into the buried pocket, thereby leading to formation of the longer polyketides (Figure 3). Most of the polyketide elongation reactions were, however, terminated at the triketide stage to yield TAL as a predominant product. A similar active-site architecture with a downward expanding polyketide tunnel has been recently reported for a bacterial pentaketide-producing type III PKS, 1,3,6,8-tetrahydroxynaphthalene synthase, from *S. coelicolor* that shares only ca. 20% amino acid sequence identity with CHS.⁹

On the other hand, Thr197 in *S. baicalensis* CHS functions as a gate keeper at the entrance of the buried pocket along with Gly211, Gln212, Leu263, Thr264, and Phe265 (Figure 3E). The replacement of Thr197 with less bulky Gly in **T197G/S338V** and **T197G/G256L/S338V** mutant widely opens the gate, thereby expanding the putative polyketide chain elongation tunnel, which led to significantly increased production of the longer chain polyketides including the octaketide SEK4/SEK4b (Figure 2A and 2B). Whereas, small-to-large substitutions in place of the residue 197 (**T197A/G256L/S338V** and **T197M/G256L/S338V**) resulted in decrease of the octaketide-forming activity and the concomitant formation of shorter chain polyketides (Figure 2A and 2B), which is well consistent with our previous reports that the residue 197 determines the polyketide chain length and product specificities in *A. arborescens* OKS^{3b} and *A. arborescens* PCS.^{3a}

Finally, the OKS- and 2PS-like bulky **G256L** substitution^{6b,9} contributes to a steric constriction of the coumaroyl binding

pocket,^{2a} thus controlling the starter substrate selectivity in *S. baicalensis* CHS (Figure 3). In fact, **G256L** and **G256L/S338V** mutant did not yield any polyketide products from the bulky coumaroyl starter (Figure 2C), but instead efficiently produced TAL from the malonyl starter (Figure 2A). It was interesting that the additional, the downward expanding, T197G replacement recovered chalcone-forming activity of the CHS mutants (**T197G/G256L** and **T197G/G256L/S338V**) (Figure 2C).

In summary, it was for the first time demonstrated that the CHS active-site can be extended to allow for the synthesis of larger polyketides including SEK4/SEK4b by a single amino acid substitution **S338V**. Further, the octaketide-forming activity was dramatically increased in the OKS-like *S. baicalensis* CHS triple mutant (**T197G/G256L/S338T**). The functional conversion is based on the simple steric modulation of a chemically inert residue lining the active-site cavity. These results provided structural basis for understanding the functional diversity of type III PKS enzymes and suggest strategies for engineered biosynthesis of plant polyketides.

Acknowledgment. This work was in part supported by the COE21 Program, Grant-in-Aid for Scientific Research (nos. 16510164, 17310130, and 17035069), Cooperation of Innovative Technology and Advanced Research in Evolutionary Area (CITY AREA), from the MEXT, Japan, and by Health and Labor Sciences Research Grant from the MHLW, Japan.

Supporting Information Available: Experimental procedures. This material is available free of charge via the Internet at <http://pubs.acs.org>.

OL052912H

(9) Austin, M. B.; Izumikawa, M.; Bowman, M. E.; Udway, D. W.; Ferrer, J.-L.; Moore, B. S.; Noel, J. P. *J. Biol. Chem.* **2004**, *279*, 45162–45174.

Active site residues governing substrate selectivity and polyketide chain length in aloesone synthase

Ikuro Abe^{1,2}, Tatsuya Watanabe¹, Weiwei Lou¹ and Hiroshi Noguchi¹

¹ School of Pharmaceutical Sciences, and the COE21 Program, University of Shizuoka, Japan

² PRESTO, Japan Science and Technology Agency, Japan

Keywords

type III polyketide synthase; chalcone synthase superfamily; aloesone synthase; chalcone synthase; engineered biosynthesis

Correspondence

I. Abe, School of Pharmaceutical Sciences, University of Shizuoka, 52-1 Yada, Shizuoka 422-8526, Japan
Tel./Fax: +81 54 264 5662
E-mail: abei@ys7.u-shizuoka-ken.ac.jp

(Received 12 October 2005, revised 7 November 2005, accepted 10 November 2005)

doi:10.1111/j.1742-4658.2005.05059.x

Aloesone synthase (ALS) and chalcone synthase (CHS) are plant-specific type III polyketide synthases sharing 62% amino acid sequence identity. ALS selects acetyl-CoA as a starter and carries out six successive condensations with malonyl-CoA to produce a heptaketide aloesone, whereas CHS catalyses condensations of 4-coumaroyl-CoA with three malonyl-CoAs to generate chalcone. In ALS, CHS's Thr197, Gly256, and Ser338, the active site residues lining the initiation/elongation cavity, are uniquely replaced with Ala, Leu, and Thr, respectively. A homology model predicted that the active site architecture of ALS combines a 'horizontally restricting' G256L substitution with a 'downward expanding' T197A replacement relative to CHS. Moreover, ALS has an additional buried pocket that extends into the 'floor' of the active site cavity. The steric modulation thus facilitates ALS to utilize the smaller acetyl-CoA starter while providing adequate volume for the additional polyketide chain extensions. In fact, it was demonstrated that CHS-like point mutations at these positions (A197T, L256G, and T338S) completely abolished the heptaketide producing activity. Instead, A197T mutant yielded a pentaketide, 2,7-dihydroxy-5-methylchromone, while L256G and T338S just afforded a triketide, triacetic acid lactone. In contrast, L256G accepted 4-coumaroyl-CoA as starter to efficiently produce a tetraketide, 4-coumaroyltriacetic acid lactone. These results suggested that Gly256 determines starter substrate selectivity, while Thr197 located at the entrance of the buried pocket controls polyketide chain length. Finally, Ser338 in proximity of the catalytic Cys164 guides the linear polyketide intermediate to extend into the pocket, thus leading to formation of the heptaketide in *Rheum palmatum* ALS.

The chalcone synthase (CHS) superfamily of type III polyketide synthases (PKSs) are structurally simple homodimeric proteins that produce basic skeletons of flavonoids as well as a variety of plant polyphenols with remarkable biological activities [1,2]. The type III PKSs of plant origin usually share 50–75% amino acid sequence identity with each other, and maintain a common 3D overall fold with an absolutely conserved Cys-His-Asn catalytic triad. The polyketide formation

reaction is thought to be initiated by starter molecule loading at the active site Cys, which is followed by sequential decarboxylative condensations of malonyl-CoA. The functional diversity of the type III PKSs derives from the differences of their selection of starter substrate, number of polyketide chain elongations, and mechanisms of the final cyclization/aromatization reactions. It has been demonstrated that the shape and volume of the active site cavity greatly influence the

Abbreviations

ALS, aloesone synthase; BNY, bisnoryangonin; CHS, chalcone synthase; CoA, coenzyme A; CTAL, 4-coumaroyltriacetic acid lactone; OKS, octaketides synthase; PCS, pentaketide chromone synthase; PKS, polyketide synthase; 2PS, 2-pyrone synthase; STS, stilbene synthase; TAL, triacetic acid lactone; TFA, trifluoroacetic acid; THNS, 1,3,6,8-tetrahydroxynaphthalene synthase.

substrate selectivity and the product chain length [1,2]. In principle, only a small modification of the active site structure is sufficient to produce dramatically different products [3].

Chalcone synthase (EC 2.3.1.74), the pivotal enzyme in the biosynthesis of flavonoids, is the well characterized type III PKS that selects 4-coumaroyl-CoA as a starter to carry out sequential condensations with three

molecules of malonyl-CoA, which is followed by Claisen-type cyclization of the enzyme-bound tetra-ketide intermediate, leading to formation of naringenin chalcone (4,2',4',6'-tetrahydroxychalcone) (Fig. 1A) [1,2]. The *in vitro* CHS enzyme reaction also yields early released derailment byproducts; bis-noryangonin (BNY) [4] and 4-coumaroyltriacytic acid lactone (CTAL) [5] (Fig. 1A). Studies of the CHS-superfamily

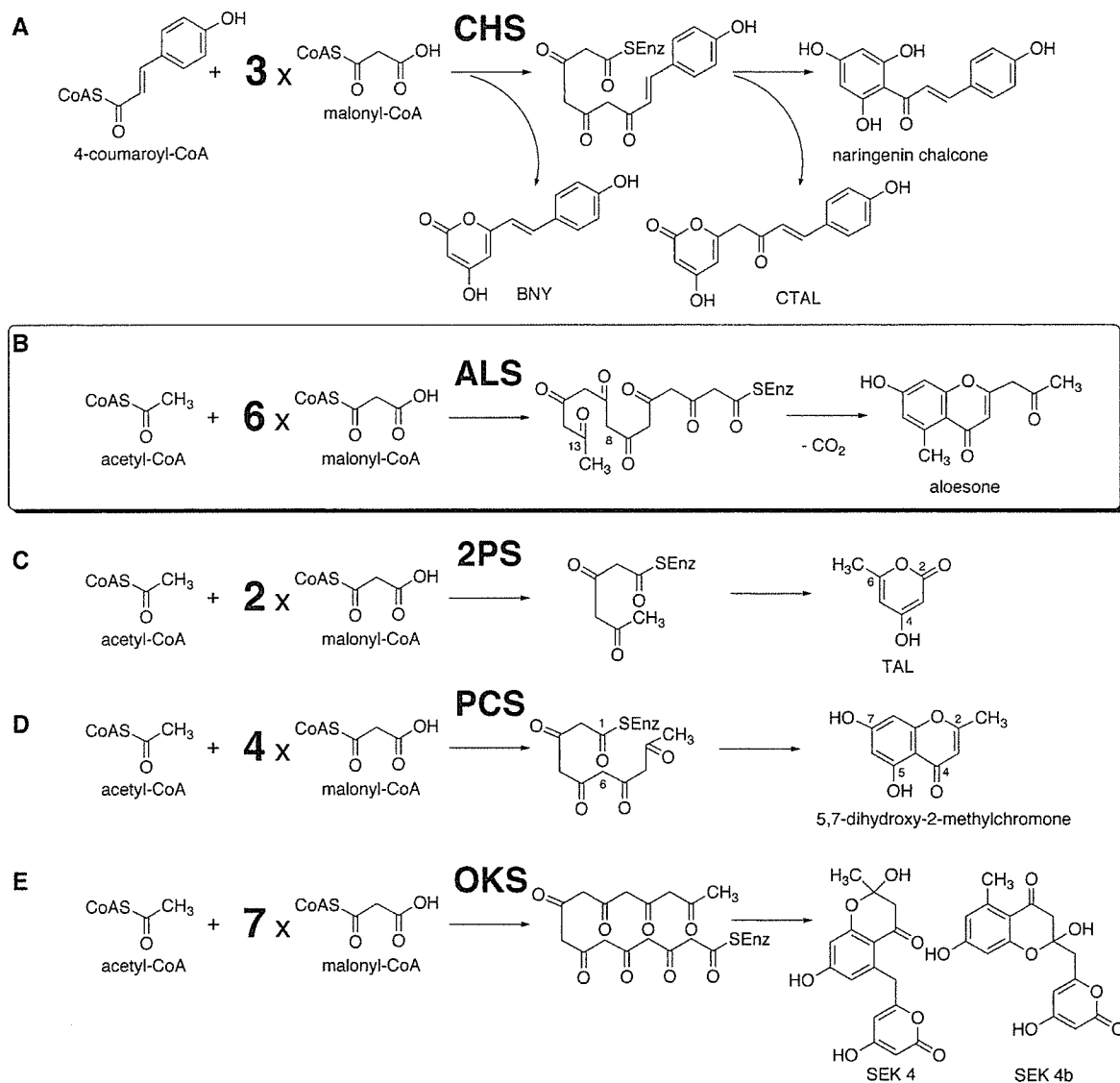


Fig. 1. Proposed mechanism for the formation of (A) naringenin chalcone from 4-coumaroyl-CoA and three molecules of malonyl-CoA by CHS (B) aloesone from acetyl-CoA and six molecules of malonyl-CoA by ALS (C) TAL from acetyl-CoA and two molecules of malonyl-CoA by 2PS (D) 5,7-dihydroxy-2-methylchromone from acetyl-CoA and four molecules of malonyl-CoA by PCS, and (E) SEK4 and SEK4b from acetyl-CoA and seven molecules of malonyl-CoA by OKS. Here BNY and CTAL are derailment by-products of the CHS reactions *in vitro* when the reaction mixtures are acidified before extraction. In PCS and OKS, acetyl-CoA, resulting from decarboxylation of malonyl-CoA, is also accepted as a starter but not so efficiently as in the case of ALS.

type III PKS enzymes are now progressing rapidly; recent crystallographic and site-directed mutagenesis studies have revealed the intimate structural details of the enzyme-catalysed processes [6–14].

On the other hand, aloesone synthase (ALS) (EC 2.3.1.-) is a novel type III PKS recently cloned from rhubarb (*Rheum palmatum*) [15], a medicinal plant rich in aromatic polyketides such as chromones, naphthalenes, phenylbutanones, and anthraquinones [16]. Aloesone synthase is the first plant-specific type III PKS that catalyses six polyketide extensions of an acetyl-CoA starter. The subsequent regiospecific C-8/C-13 aldol-type cyclization of the heptaketide intermediate and the removal of a carboxyl group from the carboxyl terminal leads to formation of aloesone (2-acetyl-7-hydroxy-5-methylchromone) (Fig. 1B). The aromatic heptaketide is known to be a biosynthetic precursor of aloesin (aloesone 8-C- β -D-glucopyranoside), the anti-inflammatory agent of the medicinal plant [15].

One of the most characteristic features of the heptaketide-producing *R. palmatum* ALS is that it lacks CHS's conserved Thr197, Gly256, and Ser338 (numbering in *Medicago sativa* CHS); the active site residues lining the initiation/elongation cavity [6] are uniquely replaced with Ala, Leu, and Thr, respectively (Fig. 2). The three residues are sterically altered in a number of functionally divergent type III PKSs including daisy (*Gerbera hybrida*) 2-pyrone synthase (2PS) (T197L/G256L/S338I) [17], aloe (*Aloe arborescens*) pentaketide chromone synthase (PCS) (T197M/

G256L/S338V) [18], and *A. arborescens* octaketides synthase (OKS) (T197G/G256L/S338V) [19]. Interestingly, these enzymes also select acetyl-CoA as a starter substrate, to carry out the decarboxylative sequential condensations with malonyl-CoA to produce triacetic acid lactone (TAL) (triketide), 5,7-dihydroxy-2-methylchromone (pentaketide), and SEK4/SEK4b (octaketides), respectively (Fig. 1).

In the TAL-producing 2PS, the three residues, 197, 256, and 338, have been shown to control starter substrate selectivity and polyketide chain length by steric modulation of the active site [20]. Indeed, a CHS triple mutant (T197L/G256L/S338I) yielded an enzyme that was functionally identical to 2PS [20]. Moreover, site-directed mutagenesis of Gly256 in CHS have established that the steric bulk at the residue 256 is important for modulating 'horizontal restriction' of the active site and thus affecting both starter and product specificity [9]. On the other hand, we have also demonstrated that residue 197 determines the polyketide chain length in the pentaketide-producing PCS and the octaketides-producing OKS from *A. arborescens*; small-to-large substitutions in place of the single residue lead to formation of shorter chain length products depending on the steric bulk of the side chain [18,19].

Here we now report homology modelling and site-directed mutagenesis studies of *R. palmatum* ALS to elucidate the functional roles of the three active site residues, Ala197, Leu256, and Thr338, in the heptaketide-producing novel type III PKS. It was demonstrated that the steric modulations of the active site

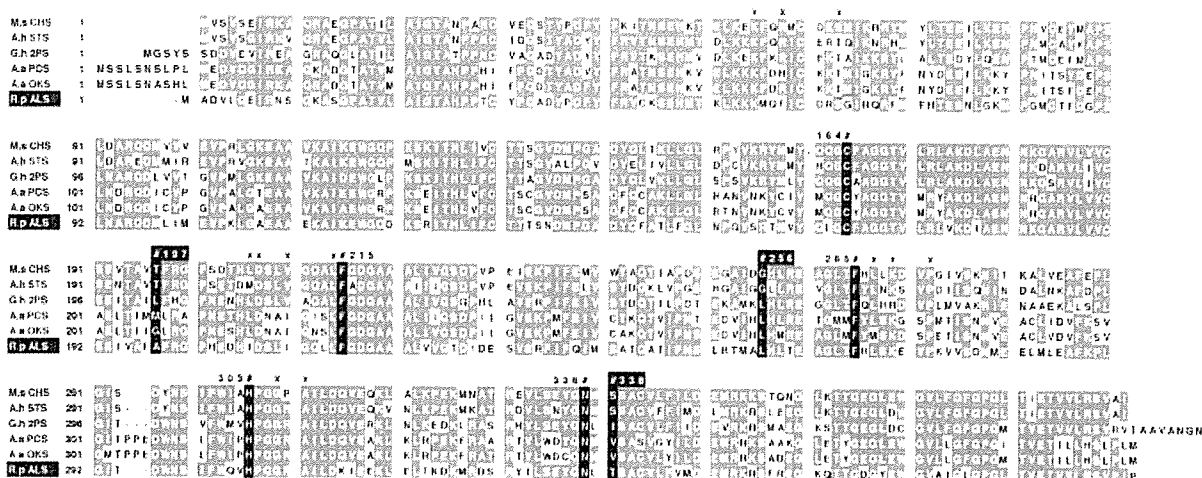


Fig. 2. Comparison of primary sequences of *R. palmatum* ALS and other CHS-superfamily type III PKSs: M.s CHS, *M. sativa* CHS; A.h STS, *Arachis hypogaea* stilbene synthase; G.h 2PS, *G. hybrida* 2-pyrone synthase; A.a PCS, *A. arborescens* PCS; A.a OKS, *A. arborescens* OKS; R.p ALS, *R. palmatum* ALS. The critical active site residues 197, 256, and 338, as well as the catalytic triad (Cys164, His303, and Asn336) and the gatekeeper Phe (Phe215 and Phe265) are highlighted. Residues for the CoA binding are marked with x.

cavity facilitates ALS to utilize the smaller acetyl-CoA starter instead of the bulky 4-coumaroyl-CoA, and to carry out the six successive condensations with malonyl-CoA to produce the hexaketide aloesone.

Results

The primary sequence of *R. palmatum* ALS exhibits 50–60% identity to those of other CHS-superfamily type III PKSs of plant origin; 62% identity (243/391) with *M. sativa* CHS [6], 69% identity (270/391) with a triketide-producing *G. hybrida* 2PS [17], 52% identity (196/391) with a pentaketide-producing *A. arborescens* PCS [18], and 52% identity (203/391) with an octaketide-producing *A. arborescens* OKS [19] (Fig. 2). In contrast, ALS showed only 21% identity (83/391) with a bacterial pentaketide-producing type III PKS, 1,3,6,8-tetrahydroxynaphthalene synthase (THNS) from *Streptomyces griseus* [21]. Sequence analysis revealed that *R. palmatum* ALS maintains almost identical CoA binding site and the catalytic triad of Cys164, His303, and Asn336 (numbering in *M. sativa* CHS) (Fig. 2). Furthermore, most of the active site residues including Met137, Gly211, Phe215, Gly216, Phe265, and Pro375 are well conserved in ALS. However, as mentioned above, CHS's Thr197, Gly256, and Ser338, the active site residues lining the initiation/elongation cavity [20], are uniquely substituted with Ala, Leu, and Thr, respectively (Fig. 2).

In the absence of a crystal structure of ALS, the CHS-based homology model predicted that the heptaketide-producing *R. palmatum* ALS has the same 3D overall fold as CHS, with the total cavity volume (1173 Å³) slightly larger than that of the pentaketide (C₁₀H₈O₄) forming PCS (1124 Å³) [18] and the tetra-ketide chalcone (C₁₅H₁₂O₅) forming CHS (1019 Å³)

[6], but much larger than that of the triketide (C₆H₆O₃) forming *G. hybrida* 2-PS (298 Å³) [17]. This suggested that the active site cavity of ALS is well large enough to perform the six rounds of the sequential condensations with malonyl-CoA and to accommodate the heptaketide product (C₁₃H₁₂O₄).

Further, as recently suggested by Noel and coworkers [22], the homology model predicted that active site architecture of ALS combines a 'horizontally restricting' (2PS and OKS-like) bulky G256L substitution with a 'downward expanding' (OKS-like) T197A replacement relative to CHS (Fig. 3). The residue 256 lining the initiation/elongation cavity indeed occupies a crucial position for the loading of the starter substrate (Fig. 4). Moreover, in the homology model, there is an additional buried pocket that extends into the traditionally solid 'floor' of the CHS active site cavity [22,23] (Fig. 4B). The large-to-small T197A replacement in ALS now opens a gate to the buried pocket, thereby expanding a putative polyketide chain elongation tunnel. Interestingly, similar active site architecture has been also recently described for a bacterial pentaketide-producing THNS from *Streptomyces coelicolor* [22] that shares only ≈20% amino acid sequence identity with the plant type III PKSs.

On the basis of these observations, we hypothesized that the steric modulations of the active site by the three residues facilitate ALS to utilize the smaller acetyl-CoA starter instead of bulky 4-coumaroyl-CoA while providing adequate volume for the heptaketide chain extensions. To test the hypothesis and to further elucidate the functions of the residues, we constructed a series of site-directed mutants at the three amino acids, Ala197, Leu256, and Thr338, in *R. palmatum* ALS (A197T, A197G, L256G, T338S, A197T/L256G, L256G/T338S, A197T/T338S, and

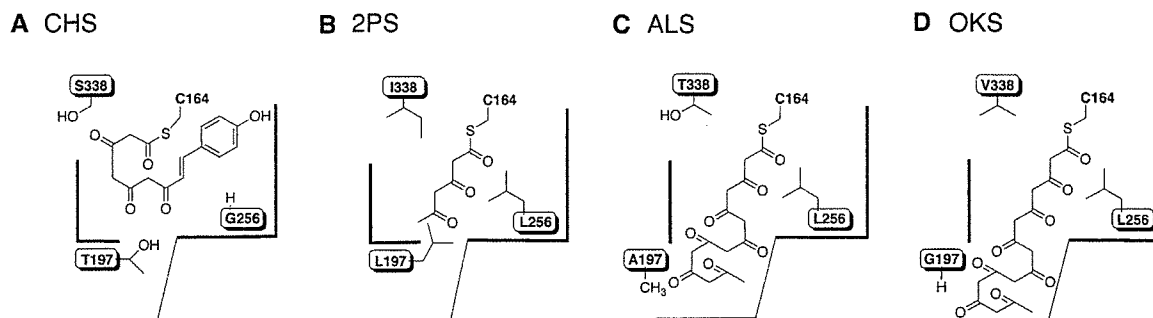


Fig. 3. Schematic representation of the active site architecture of (A) *M. sativa* CHS (B) *G. hybrida* 2PS (C) *R. palmatum* ALS, and (D) *A. arborescens* OKS (numbering in *M. sativa* CHS). The 'horizontally restricting' G256L substitution controls the starter substrate selectivity, while the 'downward expanding' substitution of T197A (ALS) and T197G (OKS) open a gate to an additional buried pocket that extends into the 'floor' of the active site cavity. On the other hand, the residue Thr338 (ALS) and Val338 (OKS) located in proximity of the catalytic Cys164 at the 'ceiling' of the active site cavity guides the growing polyketide chain to extend into the buried pocket.

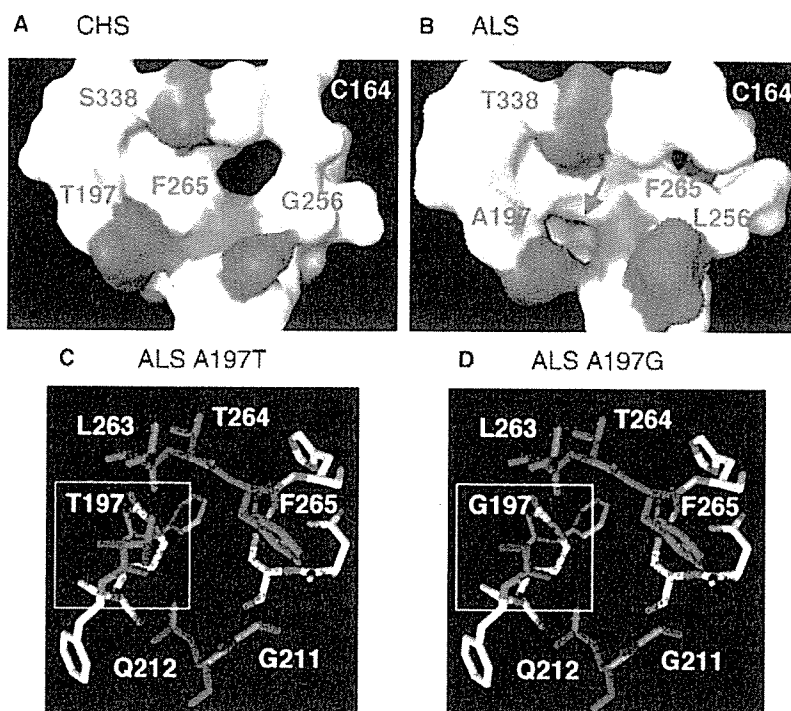


Fig. 4. (A, B) Comparison of the active site cavities of *M. sativa* CHS and *R. palmatum* ALS (each molecular surface, only includes residues lining the cavity). The three key residues 197, 256, and 338 (blue), as well as the catalytic Cys164 (yellow) and Phe265 (green) are highlighted (numbering in *M. sativa* CHS). (C) and (D); comparison of an entrance of a buried pocket that extends into the 'floor' of the active site cavity of pentaketide-producing ALS A197T and octaketides-producing ALS A197G mutant. The residue 197 is a 'gatekeeper' of the buried pocket; large-to-small substitution widely opens the entrance, leading to formation of the longer polyketides. The homology model was predicted by Swiss-PDB-Viewer software [25], and rendered with The PYMOL Molecular Graphics System [DeLano Scientific, San Carlos, CA, USA (2002)].

A197T/L256G/T338S), and investigated the mechanistic consequences of the mutations using either acetyl-CoA or 4-coumaroyl-CoA as a starter substrate.

It was remarkable that even a single amino acid substitution at these positions (A197T, L256G, and T338S) completely abolished the heptaketide-producing activity; the mutants no longer catalysed the six successive polyketide chain extensions (Figs 5 and 6). Instead, the A197T mutants (A197T, A197T/L256G, A197T/T338S, and A197T/L256G/T338S) efficiently produced a pentaketide, 2,7-dihydroxy-5-methylchromone [19], from acetyl-CoA and four molecules of malonyl-CoA (Figs 5B and 6B). Interestingly, the pentaketide is a regio-isomer of 5,7-dihydroxy-2-methylchromone ($R_t = 23.5$ min, UV: λ_{\max} 292 nm), which is produced by *A. arborescens* PCS through a C-1/C-6 Claisen-type cyclization (Fig. 1D) [18]. Whereas in ALS A197T mutant, a C-4/C-9 aldol-type cyclization of the polyketide intermediate folded in a different conformation leads to formation of 2,7-dihydroxy-5-methylchromone ($R_t = 22.7$ min, UV: λ_{\max} 308 nm) (Fig. 5B) [19]. Here it should be noted that, unlike *A. arborescens* OKS G197T mutant (numbering in *M. sativa* CHS) [19], ALS A197T mutant did not yield a hexaketide, 6-(2,4-dihydroxy-6-methylphenyl)-4-hydroxy-2-pyrone, suggesting structural difference of the active site between *R. palmatum* ALS and *A. arborescens* OKS.

The heptaketide-producing ALS ($K_M = 86.9 \mu\text{M}$ and $k_{\text{cat}} = 26.9 \times 10^{-3} \text{min}^{-1}$) [15] was thus converted to a pentaketide synthase by the single replacement of Ala197 with bulky Thr as in CHS. Steady-state enzyme kinetics analysis revealed that A197T mutant showed the $K_M = 86.4 \mu\text{M}$ and $k_{\text{cat}} = 147 \times 10^{-3} \text{min}^{-1}$ for the pentaketide-producing activity (Table 1), with a broad pH optimum within a range of 6.0–8.0. The production of the pentaketide was thus five times more efficient than that of aloesone by wild-type ALS. On the other hand, a CHS-like triple mutation (A197T/L256G/T338S) significantly reduced the yield of the pentaketide; the triple mutant showed the $K_M = 89.3 \mu\text{M}$ and $k_{\text{cat}} = 2 \times 10^{-3} \text{min}^{-1}$, which was 76-fold decreases in k_{cat}/K_M compared with the single mutant.

When Ala197 of ALS was substituted with less bulky Gly, the 'downward expanding' A197G mutation led to production of octaketides SEK4 and SEK4b (ratio 1 : 4) (Figs 5C and 6C), the longest polyketides known to be synthesized by the structurally simple type III PKS [18,19]. This was in good agreement with the previous observations that the steric bulk of the residue 197 controls the polyketide chain length in the pentaketide-producing *A. arborescens* PCS [18] and the octaketide-producing *A. arborescens* OKS [19].

As mentioned above, despite the structural similarity with CHS, *R. palmatum* ALS does not accept

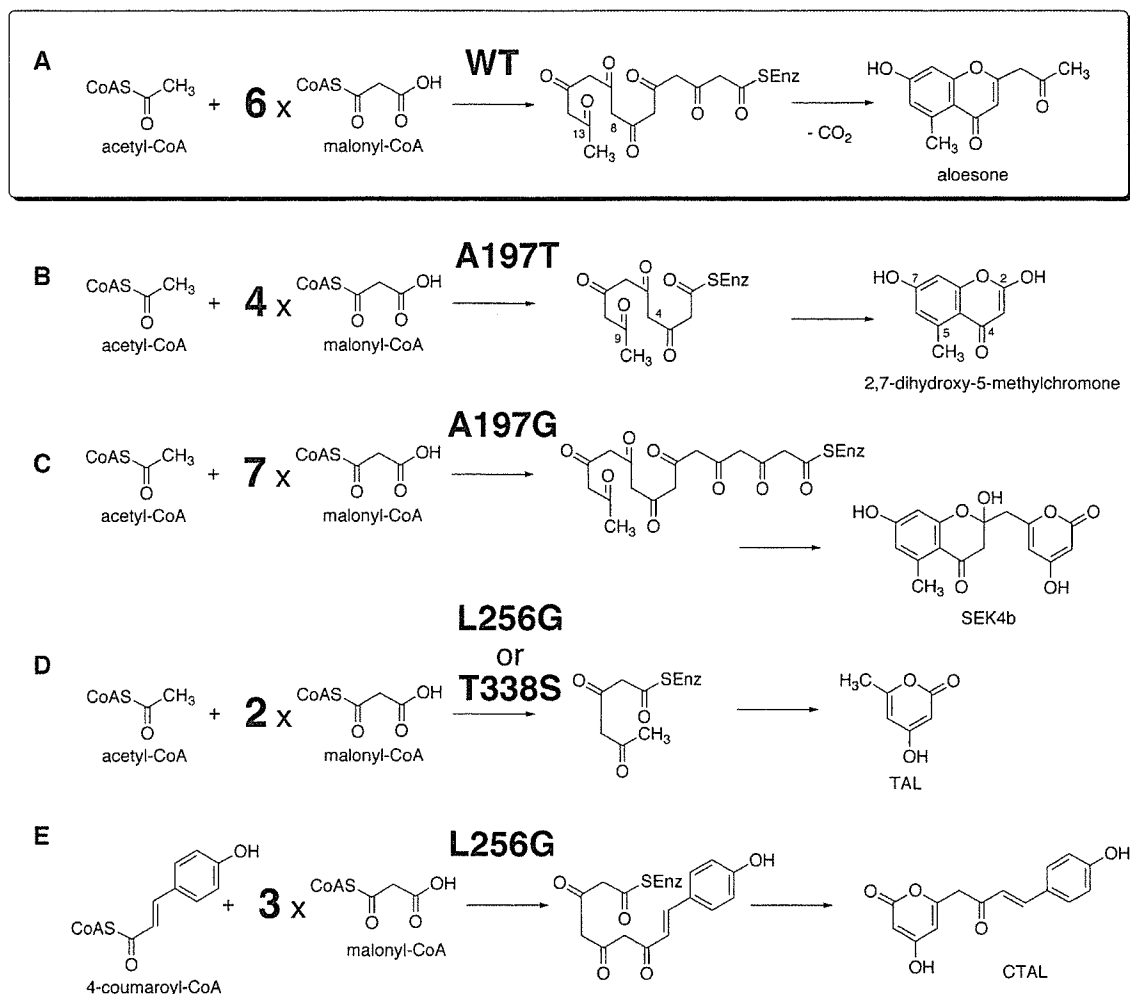


Fig. 5. Proposed mechanism for the formation of aromatic polyketides from acetyl-CoA as a starter by (A) wild-type ALS (B) ALS A197T mutant (C) ALS A197G mutant, and (D) ALS L256G or T338S mutants. The enzymes catalyse chain initiation and elongation, possibly initiating the first aromatic ring formation reaction at the methyl end of the polyketide intermediate. The partially cyclized intermediates are then released from the active site and undergo subsequent spontaneous cyclizations, thereby completing the formation of the fused ring systems. (E) Formation of CTAL from 4-coumaroyl-CoA as a starter by ALS L256G mutant.

4-coumaroyl-CoA and other aromatic CoA esters as a starter substrate for the polyketide formation reaction. However, when the 'horizontally restricting' Leu256 was substituted with small Gly as in CHS, there was a dramatic change in the enzyme reaction; ALS L256G mutant now readily accepted 4-coumaroyl-CoA as a starter to efficiently produce the tetraketide pyrone, 4-coumaroyltriacetic acid lactone (CTAL) [5] after three condensations with malonyl-CoA (Figs 5E and 6F). It was thus confirmed that the 2PS and OKS-like G256L substitution [9,20] indeed controls the starter substrate selectivity in *R. palmatum* ALS.

Interestingly, the CTAL-forming activity was dramatically increased by a combination of the CHS-like

three amino acid substitutions (A197T/L256G/T338S) (Fig. 7). Enzyme kinetics analysis revealed that ALS L256G mutant showed $K_M = 16.3 \mu\text{M}$ and $k_{\text{cat}} = 0.061 \text{ min}^{-1}$ for 4-coumaroyl-CoA, with a broad pH optimum within a range of 6.0–8.0, whereas the triple mutant exhibited $K_M = 30.1 \mu\text{M}$ and $k_{\text{cat}} = 0.336 \text{ min}^{-1}$ (Table 1), which was a threefold improvement in catalytic efficiency (k_{cat}/K_M). Further, it is noteworthy that the CTAL-forming activity is much stronger (37-fold increases in k_{cat}/K_M) than the aloesone-producing activity of wild-type ALS.

Both CTAL and chalcone formation reactions proceed through a common tetraketide intermediate (Fig. 1A). However, in the CTAL formation, the

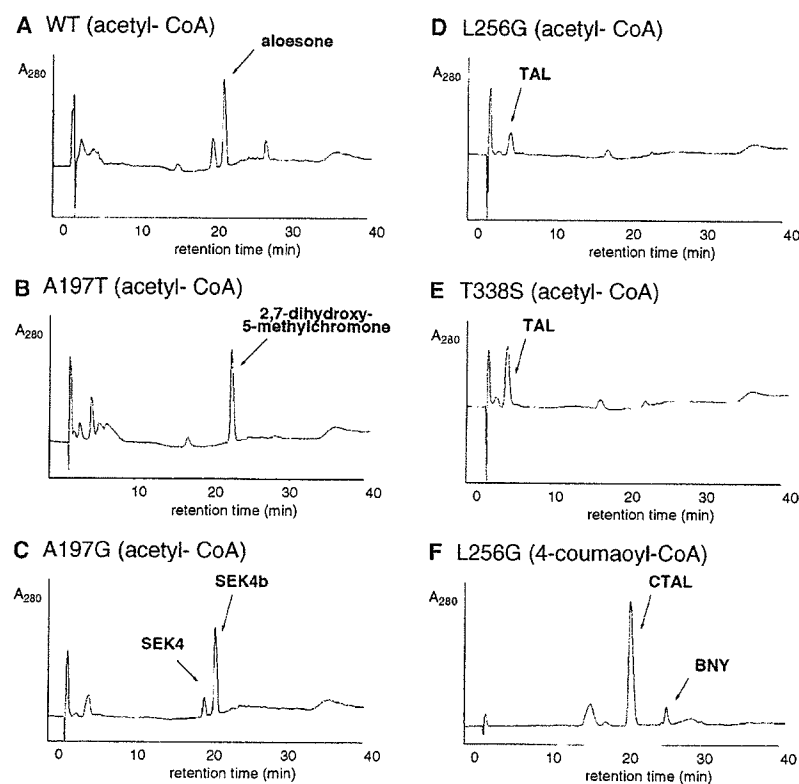


Fig. 6. HPLC elution profiles of enzyme reaction products of (A) wild-type ALS (B) ALS A197T mutant (C) ALS A197G mutant (D) ALS L256G mutant, and (E) ALS T338S mutant (acetyl-CoA as a starter). (F) ALS L256G mutant (4-coumaroyl-CoA as a starter). HPLC separation conditions were as described in Experimental procedures.

Table 1. Steady-state kinetic parameters for enzyme reactions.^a

Enzyme	Product	k_{cat} ($\times 10^{-3} \text{ min}^{-1}$)	K_M (μM)	k_{cat}/K_M ($\text{s}^{-1}\cdot\text{M}^{-1}$)
WT	Aloesone	26.9 ± 3.0	86.9 ± 4.6	5.2
A197T	2,7-Dihydroxy-5-methylchromone	147 ± 37	86.4 ± 26	28.4
A197T/L256G/T338S	2,7-Dihydroxy-5-methylchromone	2.01 ± 0.15	89.3 ± 19	0.38
L256G	CTAL	61.3 ± 7.1	16.3 ± 6.1	62.7
L256G/T338S	CTAL	168 ± 36	22.1 ± 12	127
A197/L256G	CTAL	435 ± 21	61.1 ± 7.1	119
A197T/L256G/T338S	CTAL	336 ± 20	30.1 ± 9.3	186

^aSteady state kinetic parameters were calculated for formation of major product of the enzyme reaction at optimum pH. Here kinetic parameters for the aloesone and 2,7-dihydroxy-5-methylchromone producing activities are calculated for acetyl-CoA, while for the CTAL producing activities are for 4-coumaroyl-CoA. Lineweaver-Burk plots of data were used to derive the apparent K_M and k_{cat} values (average of triplicates \pm SD) using ENZFITTER software (BIOSOFT).

enzyme reaction was terminated without construction of a new aromatic ring system. Instead, it is likely that nonenzymatic ring closure following hydrolysis of the derailed tetraketide and triketide intermediate lead to formation of the pyrone derivatives, CTAL and BNY, respectively [5]. This means that the triple mutations (A197T/L256G/T338S) were not sufficient for the functional conversion of the heptaketide-producing *R. palmatum* ALS into a chalcone-producing enzyme.

Discussion

Rheum palmatum ALS is the first plant-specific type III PKS that catalyses formation of a heptaketide aloesone. Despite the sequence similarity with CHS, ALS does not accept 4-coumaroyl-CoA as a starter substrate, but accepts acetyl-CoA to carry out the six successive condensations of malonyl-CoA (Fig. 1B). It is remarkable that formation of such a long chain polyketide is mediated by the structurally simple CHS